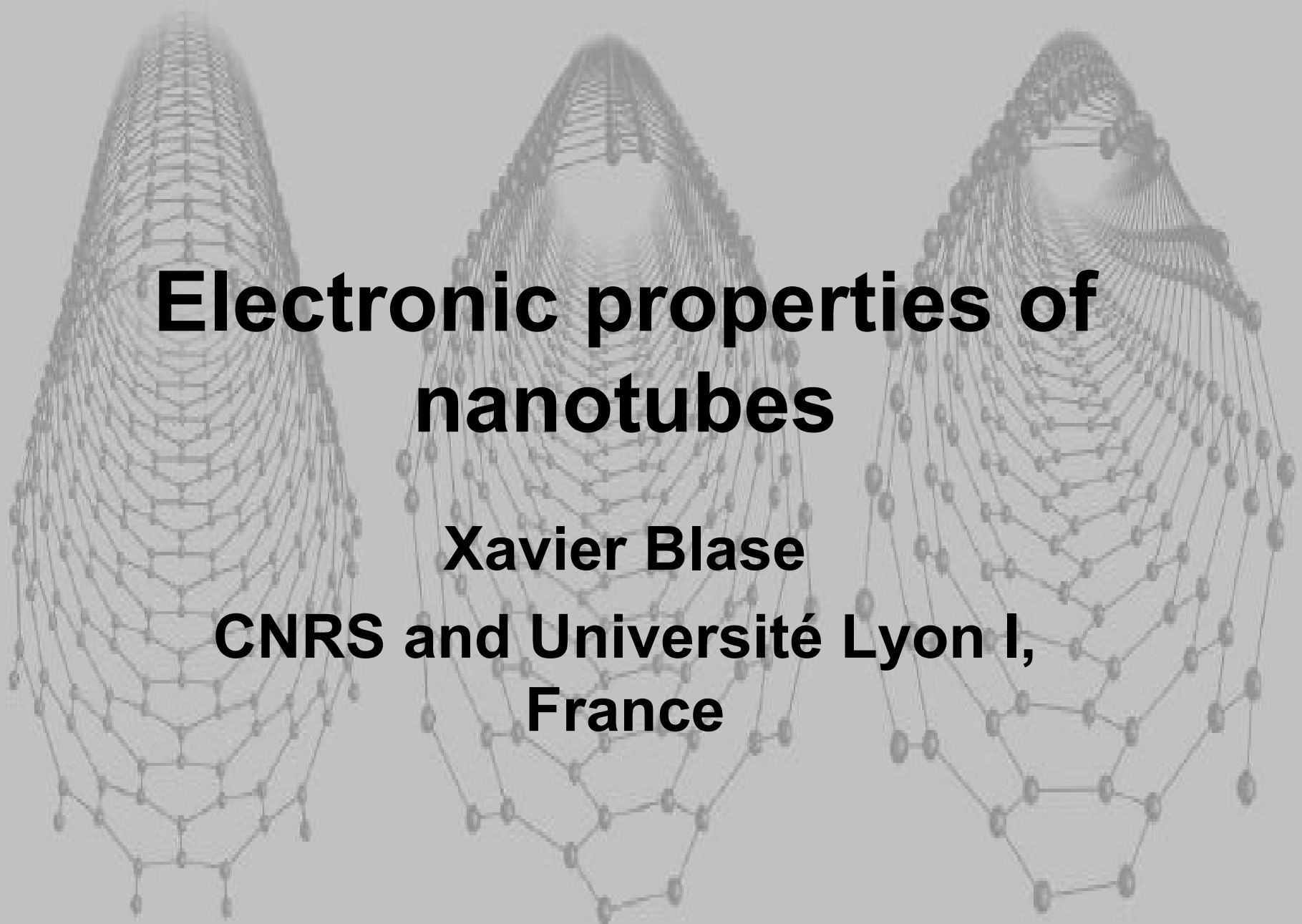


Electronic properties of nanotubes

Xavier Blase

**CNRS and Université Lyon I,
France**



Books:

- M. Endo, S. Iijima, M.S. Dresselhaus, *Carbon nanotubes*, Pergamon Press, Elsevier, 1996.
- M.S. Dresselhaus, G. Dresselhaus, P.C. Eklund, *Science of fullerenes and carbon nanotubes*, Academic Press, San Diego, California, 1996.
- T.W. Ebbesen, *Carbon nanotubes: preparation and properties*, CRC Press Inc., Boca Raton, Florida, 1997.
- R. Saito, G. Dresselhaus, *Physical properties of carbon nanotubes*, Imperial College Press, London, 1998.
- P.J.F. Harris, *Carbon nanotubes and related structures*, Cambridge University Press, Cambridge, 1999.
- D. Tománek and R.J. Enbody, *Science and application of nanotubes*, Kluwer Academic, Plenum Publishers, New York, 1999.
- S. Reich, C. Thomsen, J. Maultzsch, *Carbon nanotubes: basic concepts and Physical properties*, Wiley-VCH Verlag GmbH & Co. KGaA, Weinheim, 2004.
- A.Loiseau, P. Launois, P. Petit, S. Roche, J.-P. Salvetat, *Understanding carbon nanotubes: from basic properties to applications*, Lecture Notes in Physics 677, Springer-Verlag, Berlin, Heidelberg, 2006.

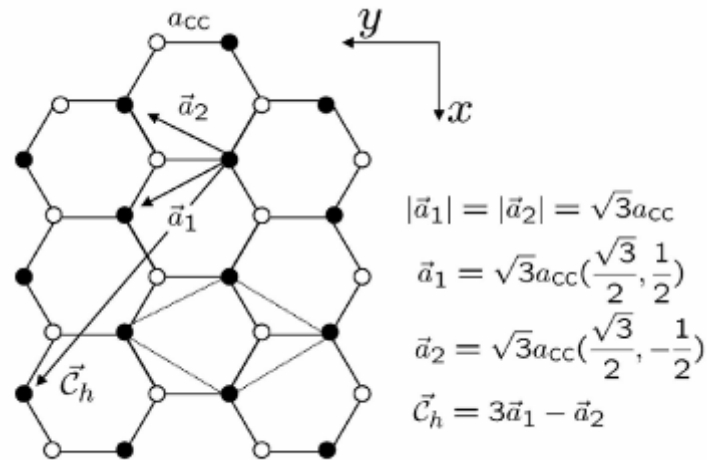
Much material in these lecture notes are extracted from:

J.-C. Charlier, X. Blase, S. Roche, « *Electronic and transport properties of nanotubes* », Rev. Mod. Phys. (submitted)

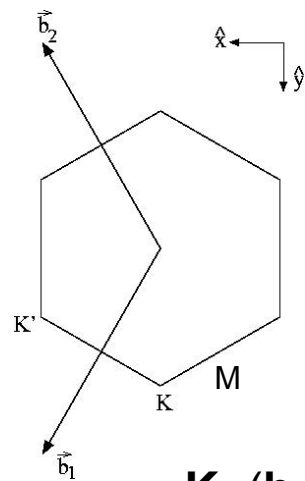
1. The graphene sheet: structure and electronic properties
 - 1a. Band structure 5-6
 - 1b. π – π^* model and tight-binding approximation 7-8
2. Making nanotubes from the graphene sheet 9-11
 - zigzag, armchair and chiral tubes
3. Electronic properties of tubes from band-folding
 - 3a. boundary conditions and allowed k-vector 12-13
 - 3b. metallic and semiconducting tubes 14
 - 3c. Armchair, zigzag and chiral tubes 15-18
 - 3d. Density of states and van Hove singularities 19-20
4. The « linear bands » approximation and consequences 21
 - 4a. the band gap depends on $1/R$ 22
 - 4b. Kataura's plot 23
 - 4c. Deviations: trigonal warping 24
5. Deviations from band folding
 - 5a. Curvature effects
 - 5a1. Secondary gaps in metallic non-armchair tubes 25-26
 - 5a2. σ – π hybridization 27
 - 5b: A note on symmetry 28
 - 5c. Bundling, multiwalls and tube-tube interactions 29

6. Beyond the independent electron approximation	
6a: Electron-phonon interaction and the Peierls transition	30
6b: Electron-phonon interaction and superconductivity	31
6c: Electron-electron and Luttinger liquid transition	32-33
7. Non-pure carbone tubes: BN and BC ₂ N tubes	
7a. Insulating BN tubes: the ionicity gap	34
7b. Photoluminescent BC ₂ N tubes	35
Addenda 1: tube-tube junctions	36

Graphene sheet: electronic structure



$$\mathbf{a}_i \cdot \mathbf{b}_j = 2\pi \delta_{ij}$$



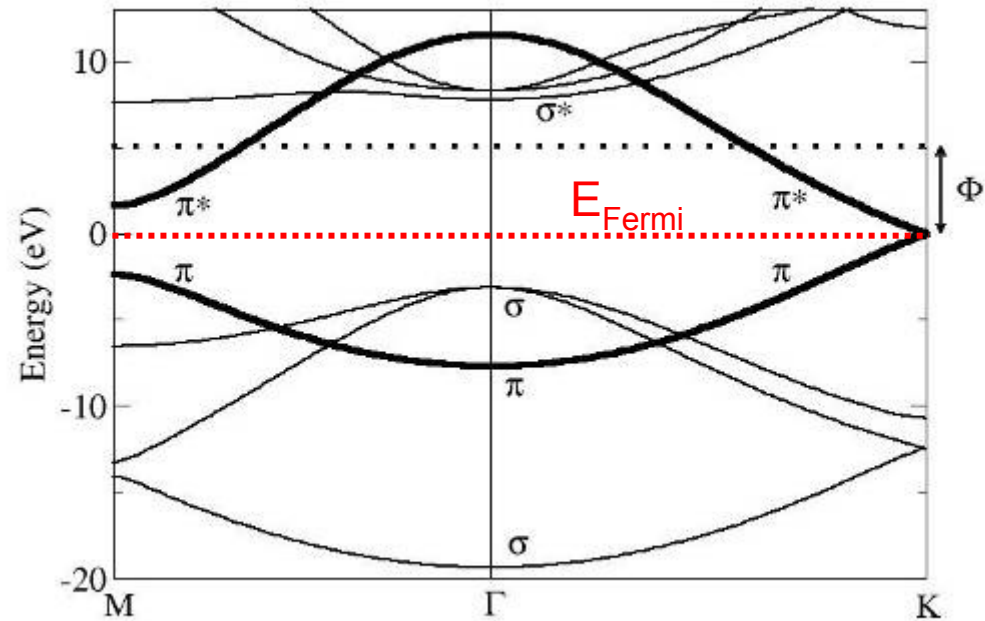
$$\mathbf{K} = (\mathbf{b}_1 - \mathbf{b}_2)/3$$

$$\mathbf{b}_1 = b(1/2, \sqrt{3}/2)$$

$$\mathbf{b}_2 = b(1/2, -\sqrt{3}/2)$$

with $b = 4\pi/a\sqrt{3}$
and $a = a_{cc}\sqrt{3}$

Graphene band structure (*ab initio*)



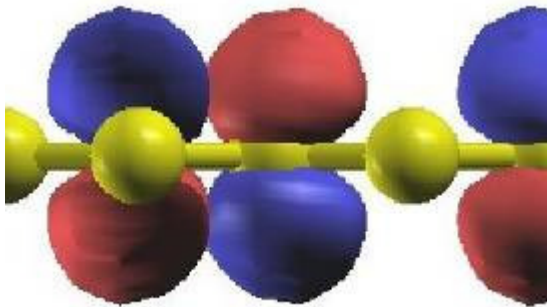
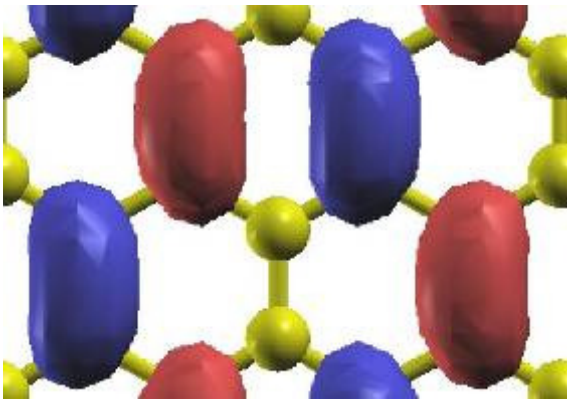
(Φ = work function (bands above are badly described))

Graphene is a semimetal with gap closing at the corners of the Brillouin zone (points K and K')

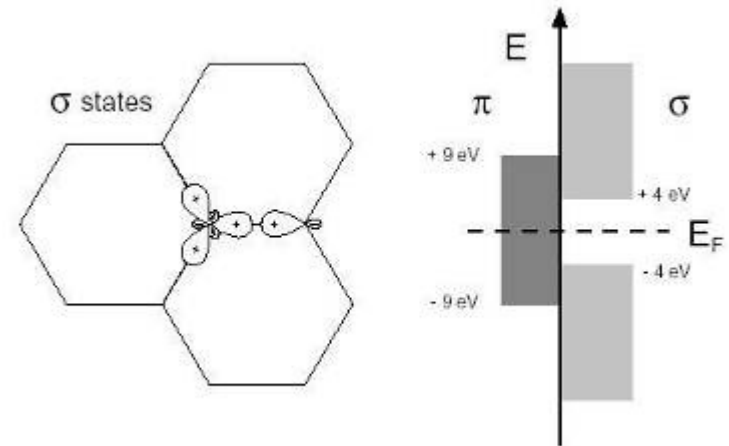
Isolated graphene sheet: Wallace, PR **71**, 622(1947);
Novoselov *et al.*, *Science* **306**, 666 (2004); Zhang *et al.*,
Nature **438**, 201 (2005).

Graphene σ and π states

π -state: linear combination of p_z orbitals
Odd with respect to graphene plane symmetry

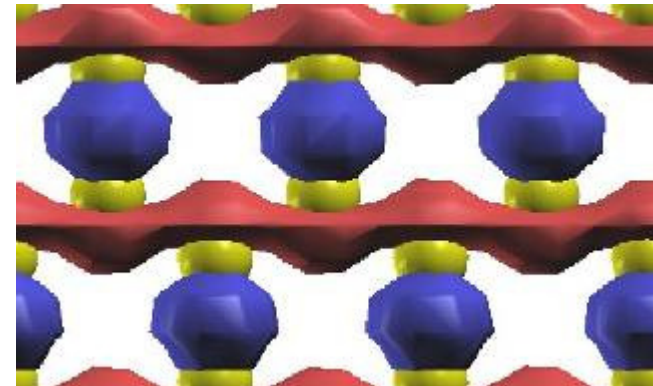


Courtesy: M.-V. Fernández-Serra



Courtesy: F. Ducastelle, Springer-Verlag 2006.

σ linear combination of s , p_x and p_y
Even with respect to planar symmetry



Red: (+) sign
Blue: (-) sign

The (orthogonal) π - π^* tight-binding model (1)

$$\Psi(\vec{k}, \vec{r}) = c_A(\vec{k})\tilde{p}_z^A(\vec{k}, \vec{r}) + c_B(\vec{k})\tilde{p}_z^B(\vec{k}, \vec{r}) \quad (\text{Bloch state})$$

$$\left\{ \begin{array}{l} \tilde{p}_z^{A/B}(\vec{k}, \vec{r}) = \frac{1}{\sqrt{N_{\text{cells}}}} \sum_{\vec{\ell}} e^{i\vec{k} \cdot \vec{\ell}} p_z^{A/B, \vec{\ell}} \quad \text{with: } p_z^{A/B, \vec{\ell}} = p_z(\vec{r} - \vec{r}_{A/B} - \vec{\ell}) \end{array} \right. \quad (\text{Bloch basis})$$

$$\det \begin{pmatrix} \mathcal{H}_{AA} - E & \mathcal{H}_{AB} \\ \mathcal{H}_{BA} & \mathcal{H}_{BB} - E \end{pmatrix} = 0 \quad \Rightarrow \quad \begin{aligned} \mathcal{H}_{AA}(\vec{k}) &= \frac{1}{N_{\text{cells}}} \sum_{\vec{\ell}, \vec{\ell}'} e^{i\vec{k} \cdot (\vec{\ell}' - \vec{\ell})} \langle p_z^{A, \vec{\ell}} | \mathcal{H} | p_z^{A, \vec{\ell}'} \rangle = \langle p_z^{A, 0} | \mathcal{H} | p_z^{A, 0} \rangle \\ \mathcal{H}_{AB}(\vec{k}) &= \frac{1}{N_{\text{cells}}} \sum_{\vec{\ell}, \vec{\ell}'} e^{i\vec{k} \cdot (\vec{\ell}' - \vec{\ell})} \langle p_z^{A, \vec{\ell}} | \mathcal{H} | p_z^{B, \vec{\ell}'} \rangle = -\gamma_0 \alpha(\vec{k}) \\ \alpha(\vec{k}) &= (1 + e^{-i\vec{k} \cdot \vec{a}_1} + e^{-i\vec{k} \cdot \vec{a}_2}) \quad \text{and: } \gamma_0 = \langle p_z^{A, 0} | \mathcal{H} | p_z^{B, 0} \rangle \end{aligned}$$

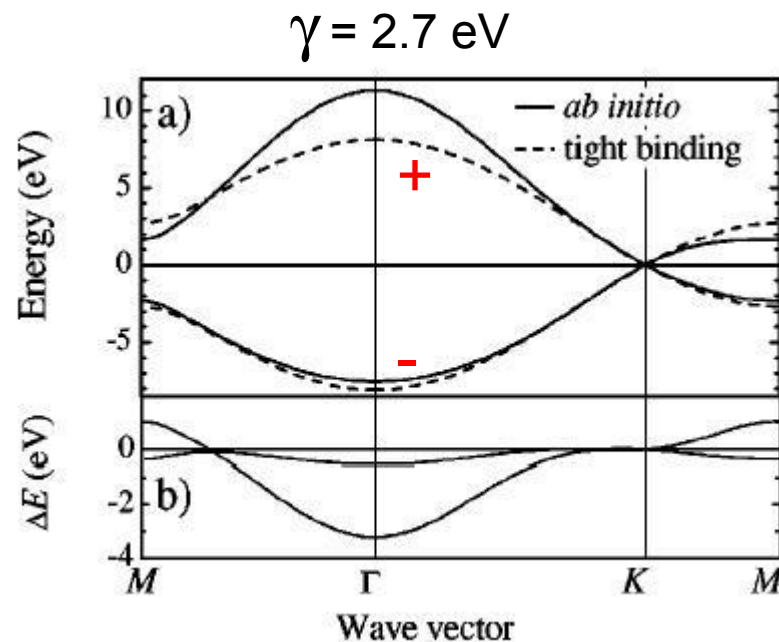
(1)

$$\begin{aligned} E_{\pm}(\vec{k}) &= \pm \gamma_0 \sqrt{3 + 2 \cos(\vec{k} \cdot \vec{a}_1) + 2 \cos(\vec{k} \cdot \vec{a}_2) + 2 \cos(\vec{k} \cdot (\vec{a}_1 - \vec{a}_2))} \\ E_{\pm}(k_x, k_y) &= \pm \gamma_0 \sqrt{1 + 4 \cos \frac{\sqrt{3} k_x a}{2} \cos \frac{k_y a}{2} + 4 \cos^2 \frac{k_y a}{2}} \quad \text{with: } \gamma_0 \sim 2.7 - 2.9 \text{ eV} \end{aligned}$$

One verifies that: $E_{\pm}(\mathbf{k}=\mathbf{K})=0$ with $\mathbf{K} = (\mathbf{a}_1 - \mathbf{a}_2)/3$

Reminder: $\cos(a+b) = \cos(a)\cos(b) - \sin(a)\sin(b)$

The (orthogonal) π - π^* tight-binding model (2)



From: Reich et al., PRB 66, 035412 (2002)

In reality, π and π^* bands are not symmetric with respect to zero energy. A better fit, including the non-zero overlap matrix elements $S = \langle p_z^A | p_z^B \rangle$, and including 2nd or 3rd nearest neighbor interaction restore this asymmetry.

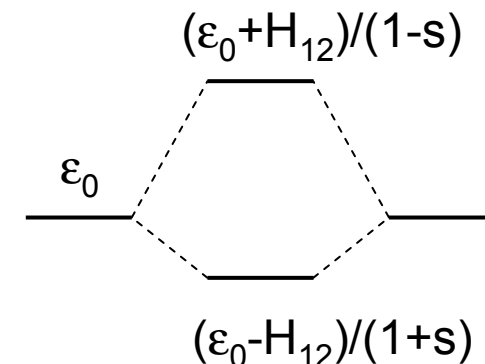
Exercise: H_2 molecule

One orbital $|s_1\rangle$ on atom 1
One orbital $|s_2\rangle$ on atom 2

Solution: $|\phi\rangle = \alpha |s_1\rangle + \beta |s_2\rangle$

Solve for eigenvalue λ :

$$|H - \lambda S| = 0 \quad H_{ij} = \langle s_i | H s_j \rangle \quad S_{ij} = \langle s_i | s_j \rangle$$



$$\epsilon_0 = \langle s_1 | H s_1 \rangle \quad \text{and} \quad s = \langle s_1 | s_2 \rangle$$

Rolling a graphene sheet onto a SW nanotube

Create a tube by cutting along OB and AB' direction and folding OB onto AB'

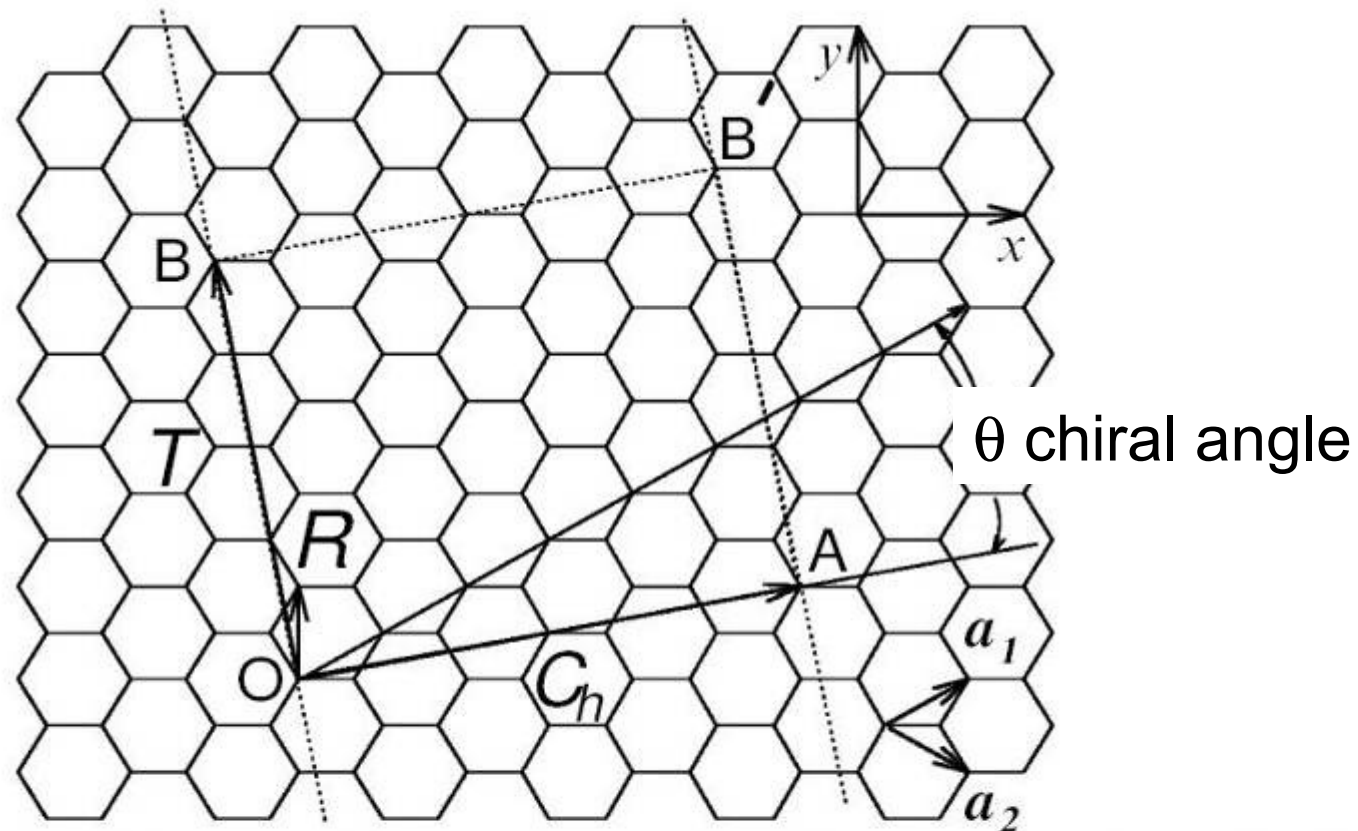
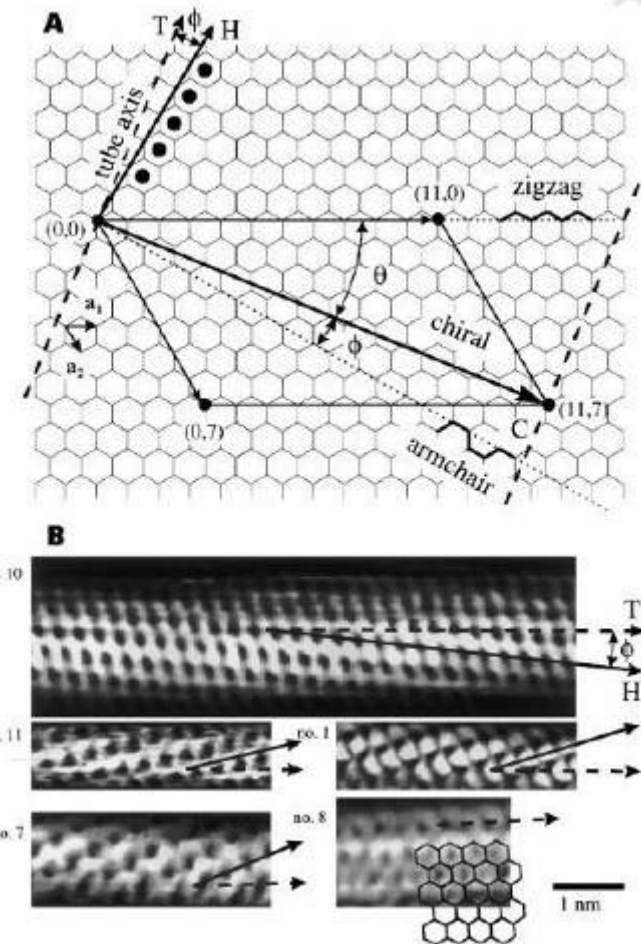
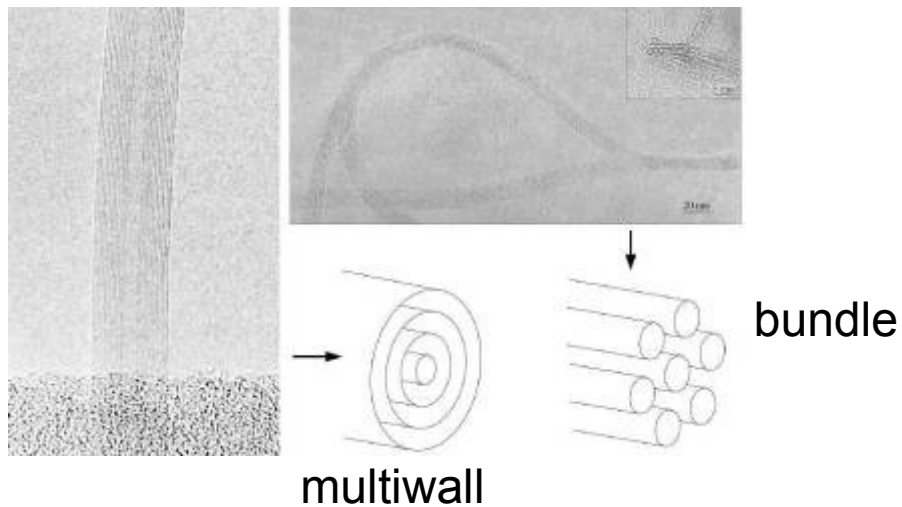
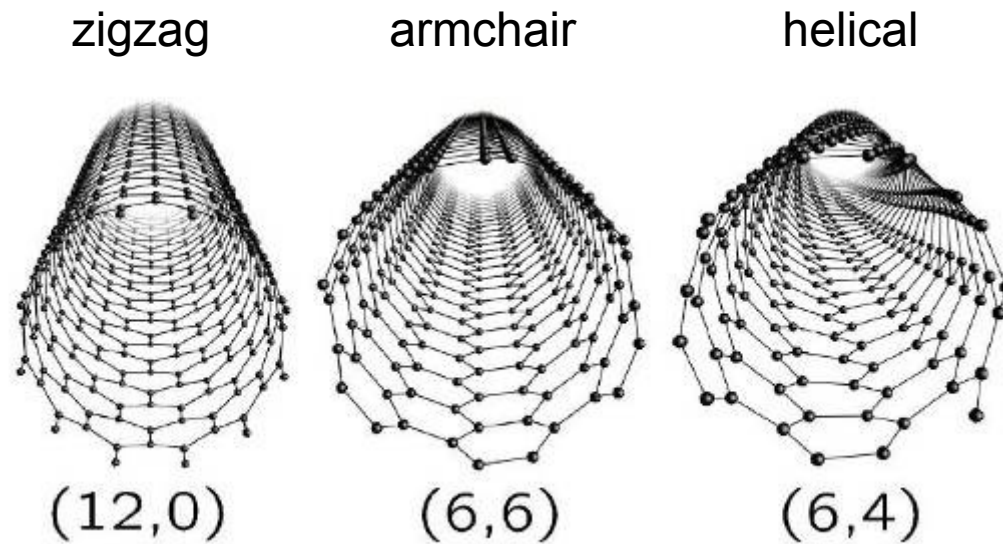


Figure 1. The unrolled honeycomb lattice of a nanotube. When we connect lattice sites O and A , and sites B and B' , a nanotube can be constructed. \vec{OA} and \vec{OB} define the chiral vector C_h and the translational vector T of the nanotube, respectively. The rectangle $OAB'B$ defines the unit cell for the nanotube. The figure is constructed for an $(n,m) = (4,2)$ nanotube [2].

Single-wall (SWNTs), multiwall (MWNTs) and bundles



(Wildöer *et al.*, *Nature* **391**, 59 (1998))

The indices (n,m) define completely the nanotube

$$\Rightarrow d_t = |\vec{C}_h| / \pi = \frac{a}{\pi} \sqrt{n^2 + nm + m^2} \quad \text{diameter}$$

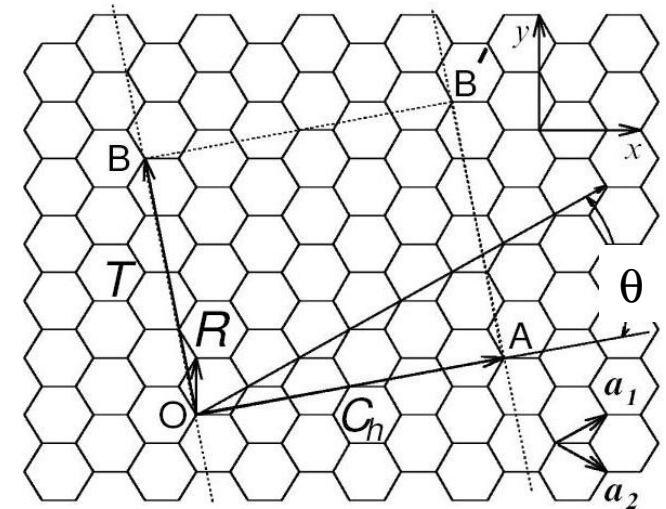
$$\Rightarrow \mathbf{T} = t_1 \mathbf{a}_1 + t_2 \mathbf{a}_2, \quad t_1 = (2n+m)/N_R \text{ and } t_2 = (2m+n)/N_R$$

N_R largest common divisor of $(2n+m)$ and $(2m+n)$

$$\Rightarrow t = |\vec{T}| = \sqrt{3}a \sqrt{n^2 + nm + m^2} / N_R \quad \text{Unit cell length along axis}$$

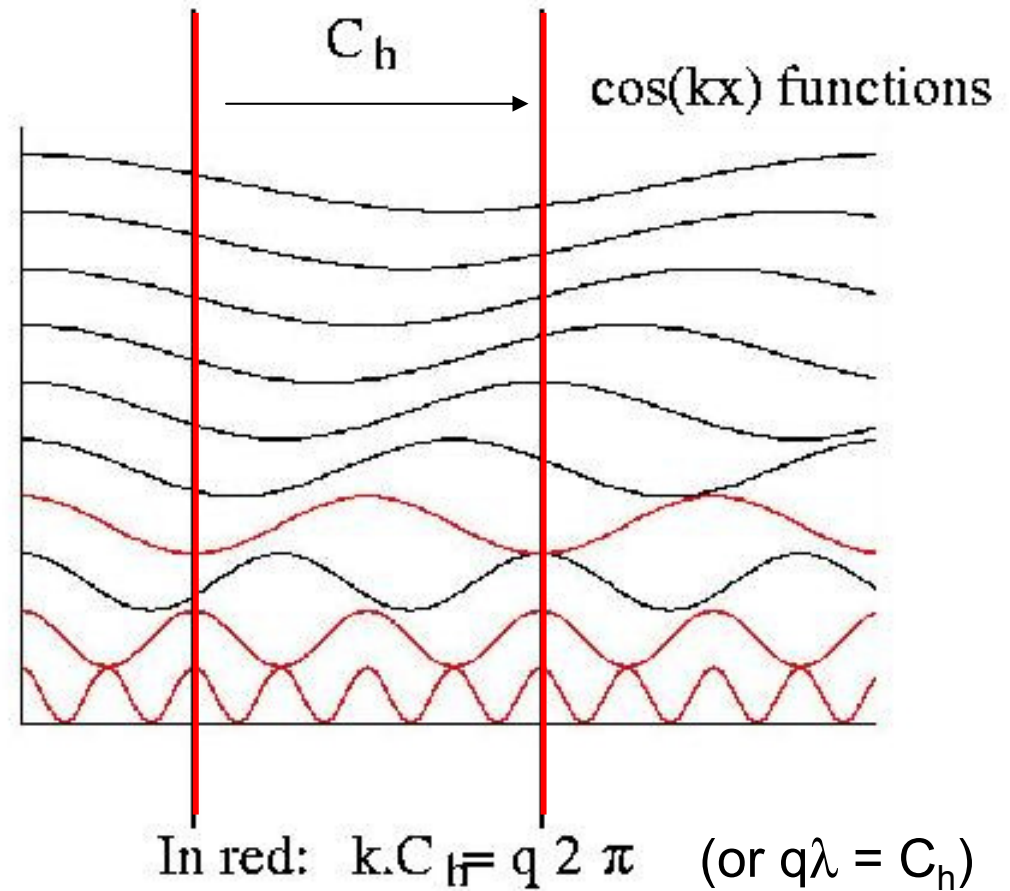
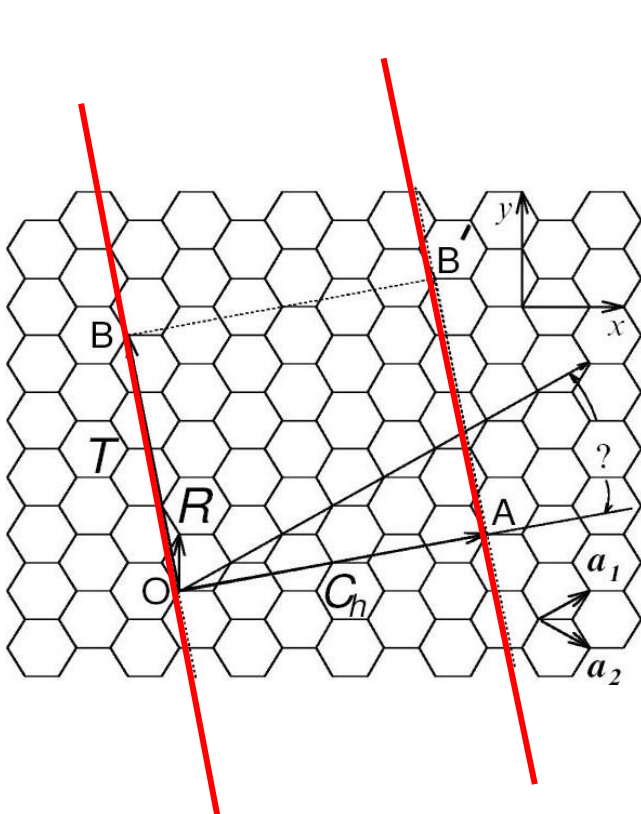
$$\Rightarrow N_C = 4(n^2 + nm + m^2) / N_R \quad \text{Number of atoms in unit cell}$$

$$\Rightarrow \cos \theta = \frac{\vec{C}_h \cdot \vec{a}_1}{|\vec{C}_h| |\vec{a}_1|} = \frac{2n+m}{2\sqrt{n^2 + nm + m^2}} \quad \text{Chiral angle (cosine)}$$



Zone-folding and k-vector selection (schematic)

The wavefunctions must be single-valued around the tube circumference:



Graphene bands selection and folding

The boundary conditions around the tube circumference (wavefunctions single valued) imposes the condition

$$\Phi_{\mathbf{k}}(\mathbf{r} + \mathbf{C}_h) = e^{i\mathbf{k} \cdot \mathbf{C}_h} \Phi_{\mathbf{k}}(\mathbf{r}) = \Phi_{\mathbf{k}}(\mathbf{r})$$



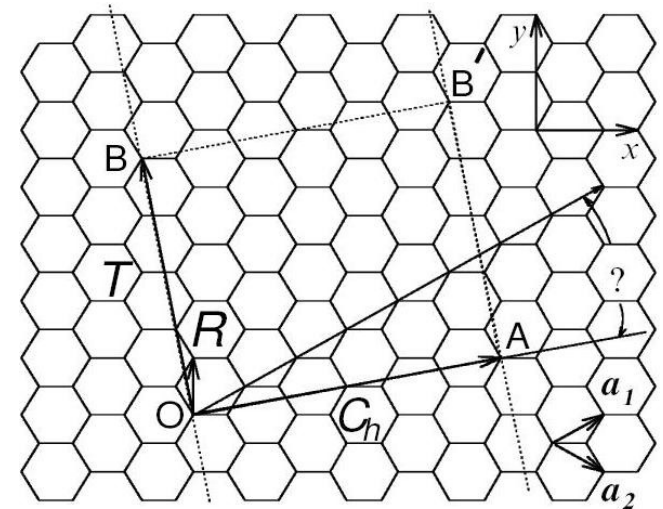
Bloch relation

$$\mathbf{k} \cdot \mathbf{C}_h = 2\pi q, q \text{ integer}$$

Defines parallel lines of allowed \mathbf{k} -vector with $2\pi/C_h$ spacing in reciprocal space:

$$\mathbf{k}^{\text{allowed}} = q \mathbf{B}_1 + k_{\perp} \mathbf{B}_2, -\pi/T < k_{\perp} < \pi/T$$

$$\begin{aligned} \mathbf{A}_1 &= \mathbf{C}_h \text{ and } \mathbf{A}_2 = \mathbf{T} \\ \mathbf{B}_i^* \mathbf{A}_j &= 2\pi \delta_{ij} \end{aligned}$$

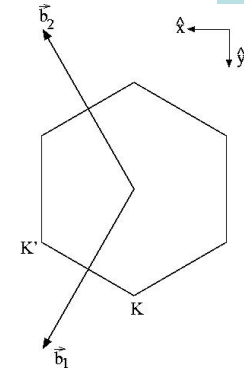


Nanotubes can be either metallic or semiconducting

$\mathbf{K} = (\mathbf{b}_1 - \mathbf{b}_2)/3$ (corner of the hexagonal BZ with zero gap)

$\mathbf{C}_h = n\mathbf{a}_1 + m\mathbf{a}_2$ and $\mathbf{a}_i \cdot \mathbf{b}_j = 2\pi \delta_{ij}$

$\mathbf{K} \cdot \mathbf{C}_h = 2\pi (n-m)/3 \Rightarrow$ if $(n-m)=3l$, l integer then \mathbf{K} is allowed



$(n-m)=3l$, l integer \Rightarrow metallic tubes

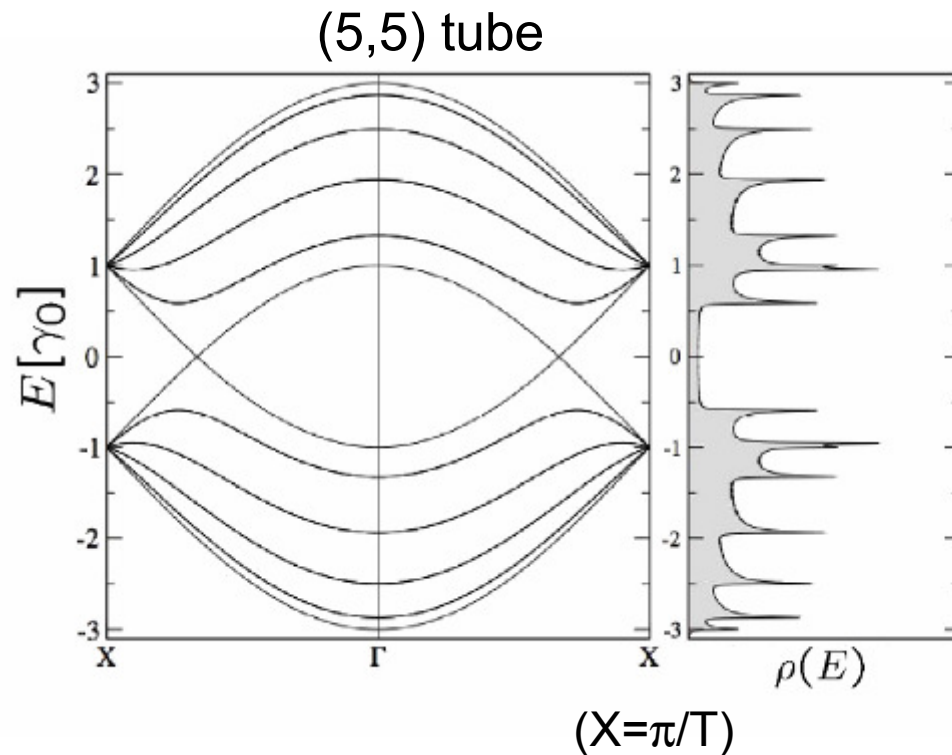
$(n-m)=3l \pm 1 \Rightarrow$ semiconducting tube

- Armchair tubes are always metallic
- Zigzag $(n,0)$ tubes are metallic if n multiple of 3
 \Rightarrow e.g. $(12,0)$ is metallic, $(13,0)$ is semiconducting

1/3 of tubes are metallic, 2/3 are semiconducting

Armchair (n,n) tubes (π - π^* band folding model)

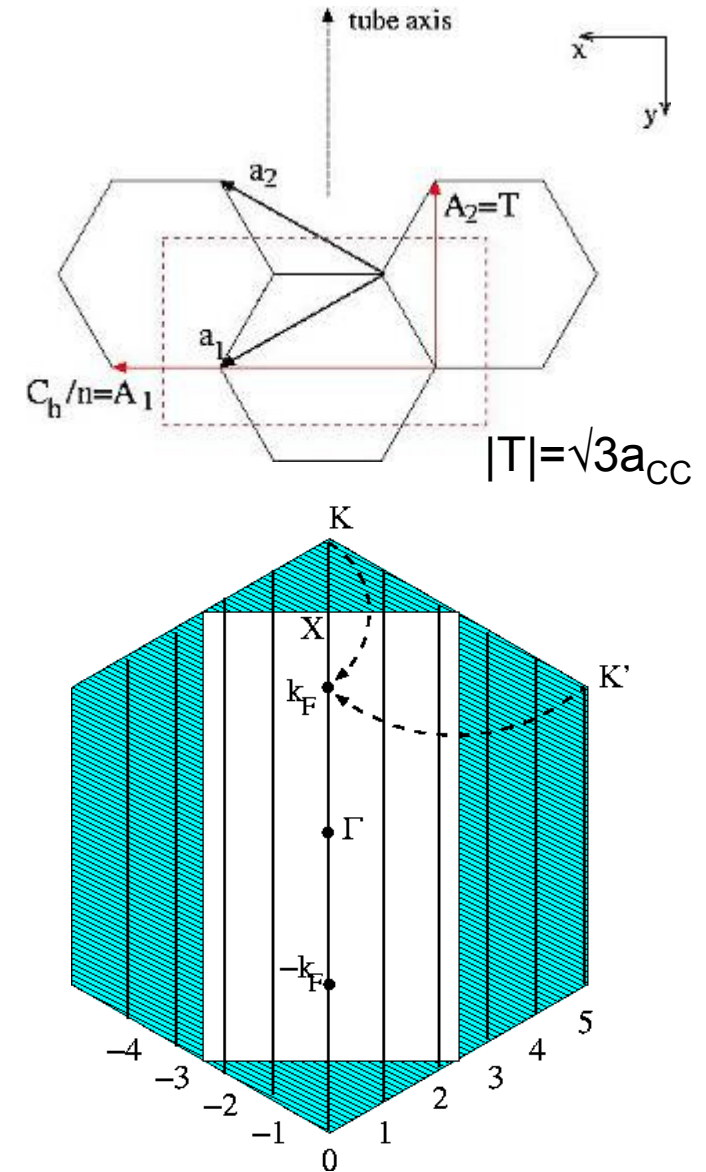
15



In armchair tubes, k_F occurs at $2/3$ of ΓX (where K is folded)

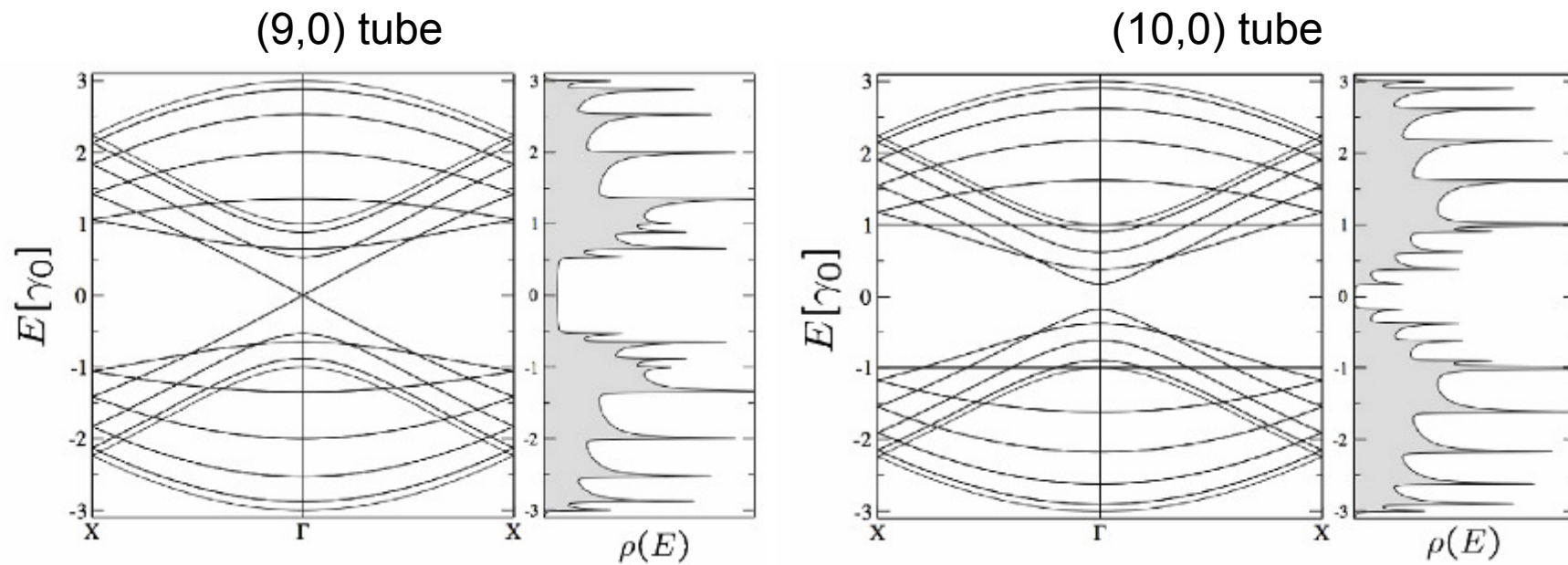
In a metallic tube, at the Fermi level:

$$\rho(\varepsilon_F) = 2\sqrt{3}a_{cc}/(\pi\gamma_0|\vec{C}_h|)$$

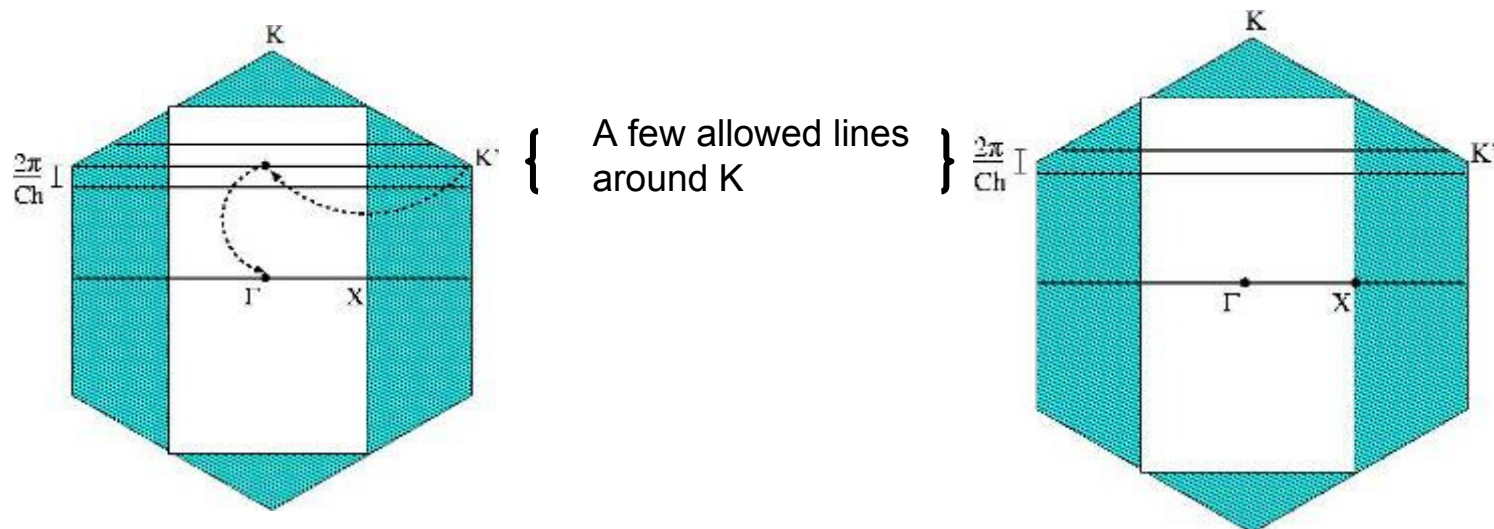


In white, BZ associated with C_h/n and T

Zigzag (n,0) tubes (π - π^* band folding model)

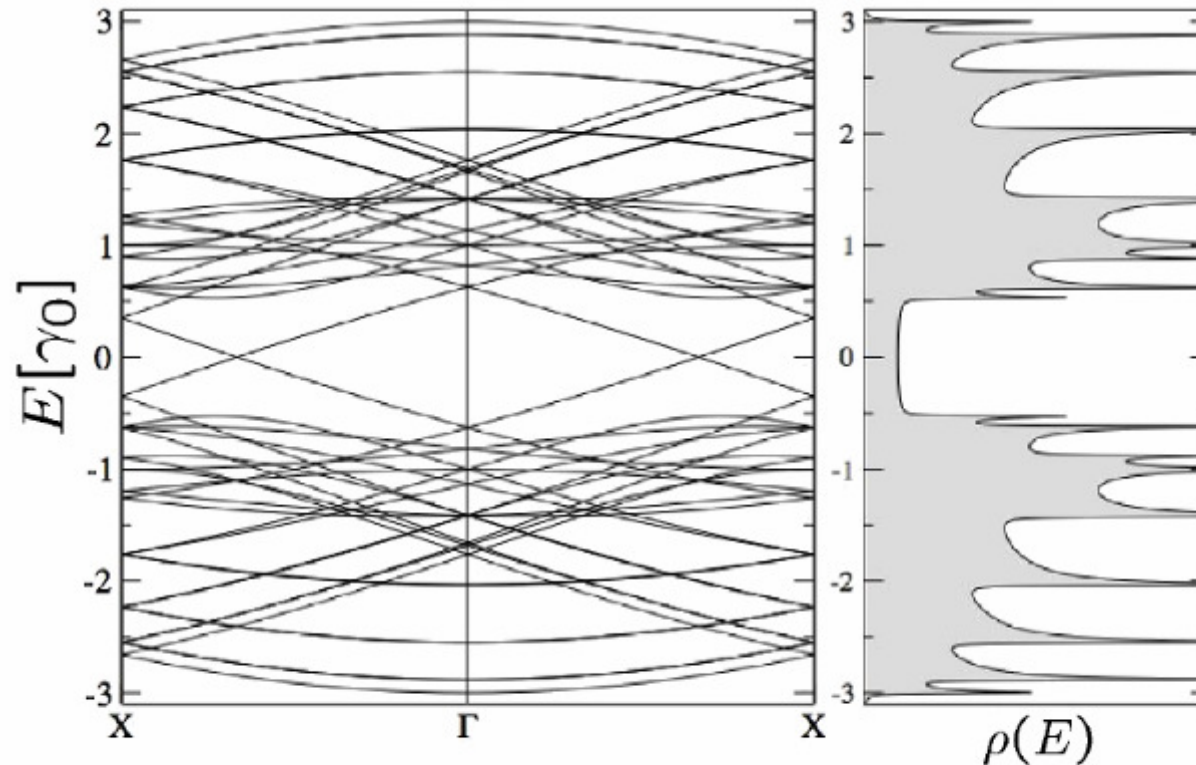


The band gap (zero when n is multiple of 3) is at zone-center Γ



Chiral tubes (π - π^* zone-folding model)

(8,2) tube



In the general case of achiral ($n \neq m \neq 0$) tubes, the band gap (which can be zero if $n-m=3l$) occurs at Γ or $2/3 \Gamma X$ as well

Charlier, Lambin, PRB **57**, R15037 (1998)
 Reich, Thomsen, PRB **62**, 4273 (2000)

Comparing band folding and ab initio calculations

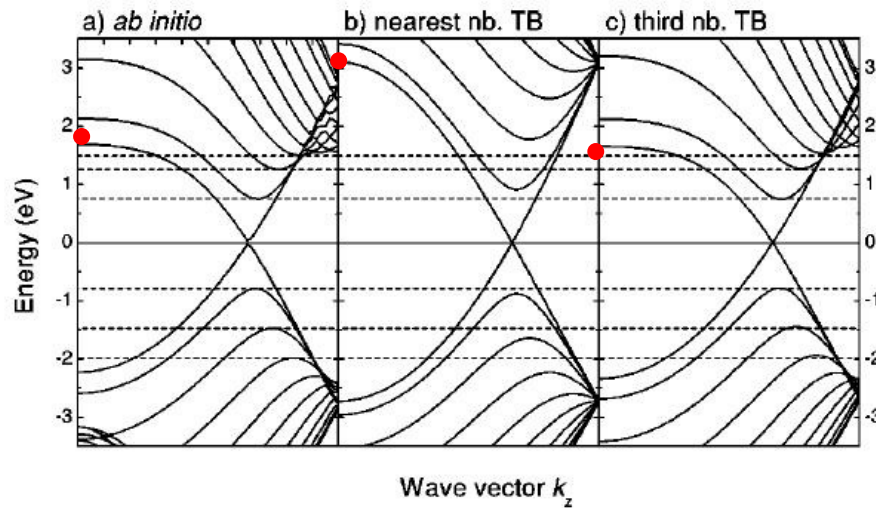


FIG. 4. Band structure of a (10,10) armchair nanotube. (a) *Ab initio* calculation. (b) Nearest-neighbor tight-binding calculation with $\gamma_0 = -2.7$ eV. (c) Third-nearest-neighbor tight-binding calculation with parameters obtained from a fit to the optical energy range; see Table I. The dashed lines denote *ab initio* calculated energies of the singularities in the density of states.

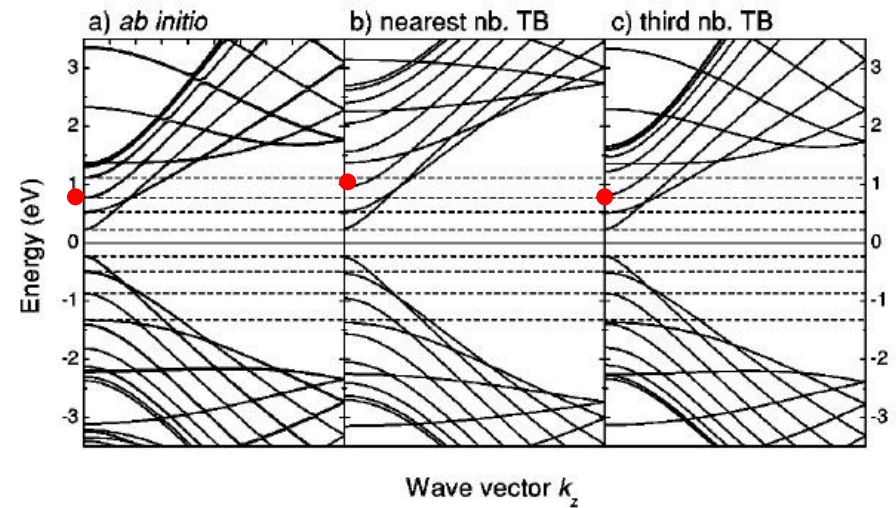


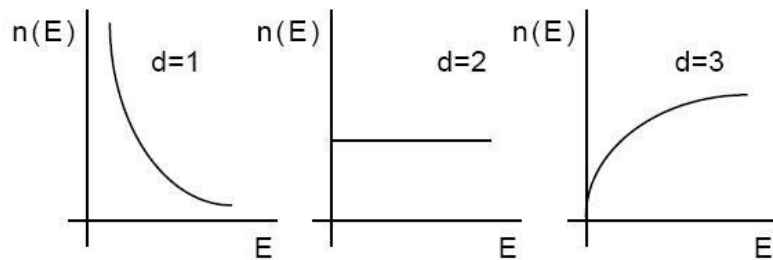
FIG. 5. Band structure of a (19,0) zigzag nanotube. (a) *Ab initio* calculation. (b) Nearest-neighbor tight-binding calculation with $\gamma_0 = -2.7$ eV. (c) Third-nearest-neighbor tight-binding calculation with parameters obtained from a fit to the optical energy range; see Table I. The dashed lines denote *ab initio* calculated energies of the singularities in the density of states.

TB=tight-binding=band folding of graphene as described with TB calculations

Electronic density of states (eDOS) in 1,2 and 3D. van Hove singularities

The density of states $\rho(E)$ - which gives the number of states $\rho(E)dE$ per energy span dE - is proportional to $1/\sqrt{E}$ close to a band extrema ($dE/dk=0$) in 1D

Behavior of DOS close to a band extremum or saddle-point ($\nabla_{\mathbf{k}}(E)=0$) in 1D, 2D and 3D:



(graph from: Loiseau et al., Understanding carbon Nanotubes, Lecture Notes in Physics **677**, Springer-Verlag, 2006)

$\nabla_{\mathbf{k}}(E)=0$ defines the « critical points » in the BZ with:

$$\rho(E) \sim \int dS / |\nabla_{\mathbf{k}} E|$$

(S =constant energy surface):

$$\begin{aligned} \rho(E) &= \frac{2}{\Omega} \sum_q \sum_{s=\pm} \int dk \delta(E - E_q^s(k)) \quad (k=k_z=k_{\parallel}) \\ &= \frac{2}{\Omega} \sum_q \sum_{s=\pm} \int dk \delta(k - k_{qs}) \times \left| \frac{\partial E_q^s(k)}{\partial k} \right|^{-1} \end{aligned}$$

with: k_{qs} roots of $E - E_q^s(k)=0$. Using linearity of bands (see next page), one finds:

$$\left| \frac{\partial E_q^s(k)}{\partial k} \right|^{-1} = \frac{2}{\sqrt{3}\gamma_0 a} \frac{|E_q^s(k)|}{\sqrt{(E_q^s(k))^2 - \varepsilon_{qs}^2}}$$

$$\text{with: } \varepsilon_{qs} = \pm \pi \gamma a_{CC} |3q-n+m|/C_h$$

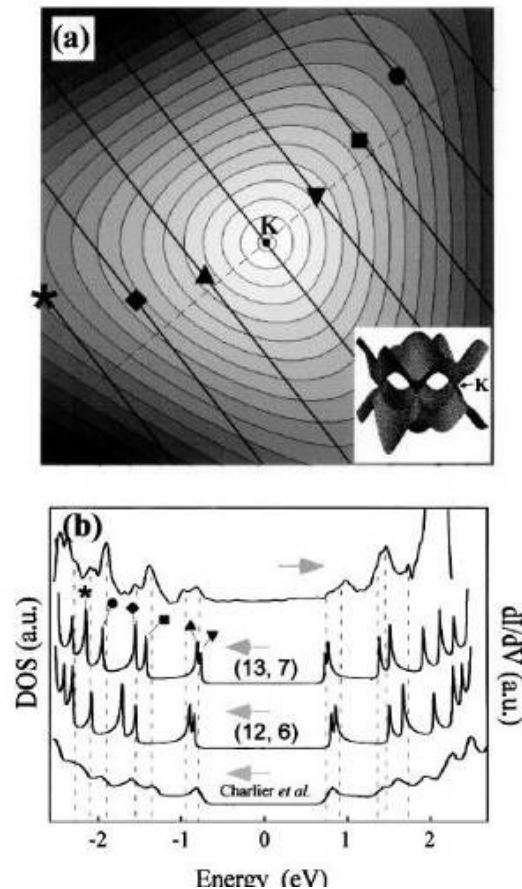
If $(3q-n+m)=0$ (metallic tube), $\varepsilon_{qs}=0$ and $\rho(E=0)=2a/\pi\gamma|C_h|$ ($a=\sqrt{3} a_{CC}$)

The $1/\sqrt{E}$ divergencies in the eDOS are called the van Hove singularities.

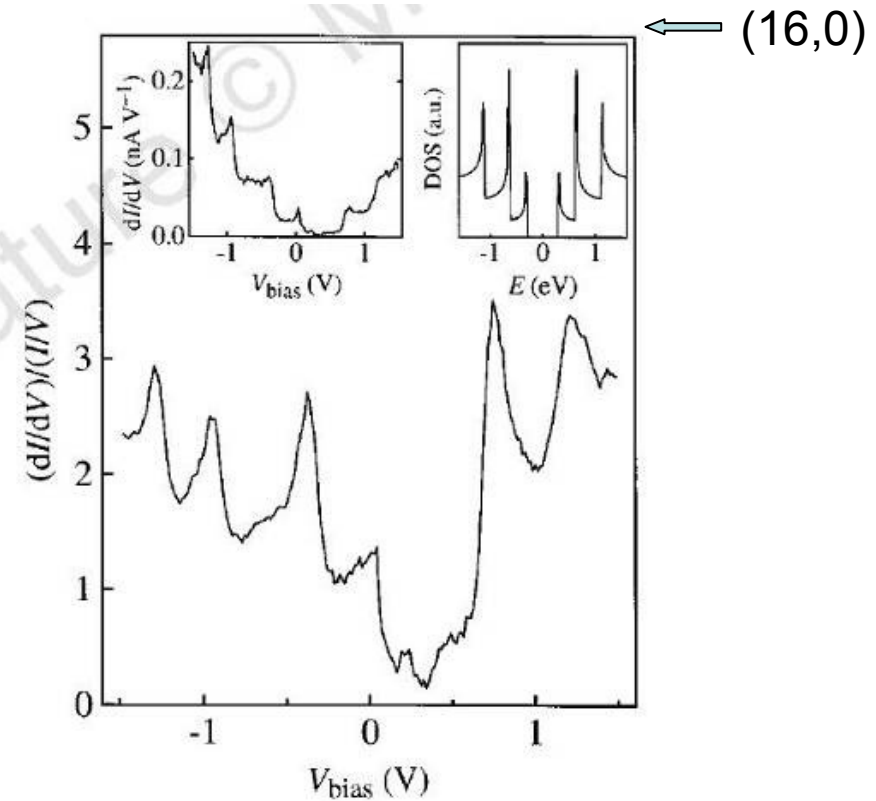
Reminder: $\delta(g(x)) = \sum_{x_0} \delta(x-x_0)/g'(x_0)$, x_0 roots of $g(x)=0$

Experimental STS measurements of eDOS

The eDOS is roughly proportional to $(dI/dV)(V/I)$ in a STS measurement. This has allowed experimental verification of the vHs structuration of the eDOS of nanotubes



Kim *et al.*, PRL **82**, 1225 (1999)



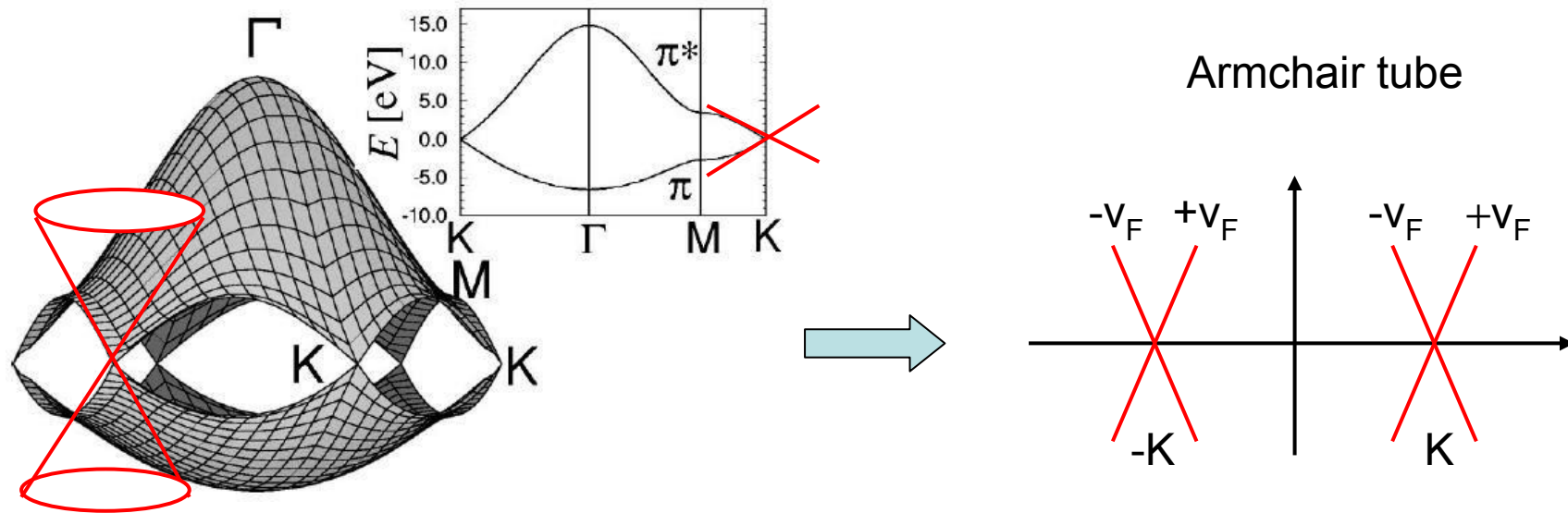
Wildöer *et al.*, *Nature* **391**, 59 (1998)

+ Odom *et al.*, *Nature* **391**, 62 (1998); Venema *et al.*, PRB **62**, 5238 (2000); Avramov *et al.*, CPL **370**, 597 (2003)

The approximation of linear bands around k_F and its consequences

21

(Fig: Saito et al., PRB **61**, 2981 (2000))



In the vicinity of $\mathbf{K}=(\mathbf{b}_1-\mathbf{b}_2)/3$, one writes: $\mathbf{k}=\mathbf{K}+\delta\mathbf{k}=(\delta k_x, 4\pi/3a+\delta k_y)$ and a Taylor expansion of Eq.(1) yields for a metallic tube:

$$E_{\pm}(\delta k) \simeq \pm \frac{\sqrt{3}a}{2}\gamma_0 \parallel \delta \vec{k} \parallel \quad \underline{\underline{v=\nabla_{\mathbf{k}}E/\hbar}} \quad v_F = \sqrt{3}a\gamma_0/2\hbar = \frac{3}{2}a_{cc}\gamma_0/\hbar \quad (\sim 8.10^5 \text{ms}^{-1})$$

In the case of a semiconducting tube, the Taylor expansion of (1) with the condition $\delta \vec{k} = (2\pi/|C_h|)(q \pm 1/3)\vec{\kappa}_{\perp} + k\vec{\kappa}_{\parallel}$ yields:

$$E_q^{\pm}(\delta \vec{k}) \simeq \pm \frac{\sqrt{3}a}{2}\gamma_0 \sqrt{\left(\frac{2\pi}{|C_h|}\right)^2 \left(q \pm \frac{1}{3}\right)^2 + k^2}$$

First paper (graphene): Wallace, PR **71**, 622(1947).

Linearity of bands : the band gap is inversely proportional to diameter

From the previous equation, in a semiconducting tube:
(d_t tube diameter)

$$\Delta E_g^1 = \frac{2\gamma_0 a_{cc}}{d_t}$$

Similar results can be obtained for energy gaps between
vHs in the eDOS => universal eDOS functional form

In particular, E_{22}/E_{11} ($E_{11} = \Delta E_g^1$) ratio is equal to two in this
« linear approximation ».

These results hold for large tubes (and therefore small gaps)
so that the « allowed lines » come close to the K-points in the
BZ zone.

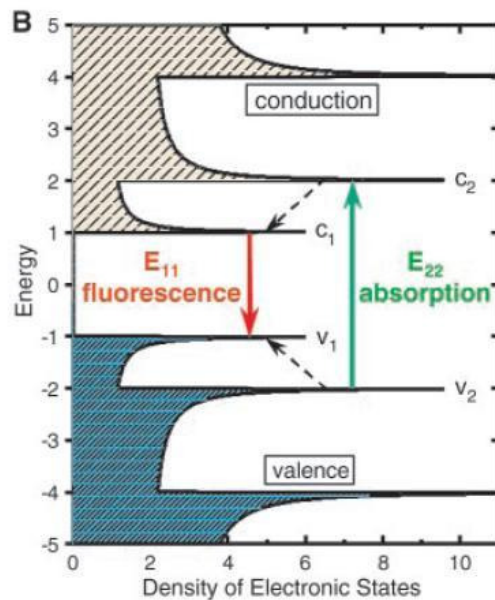
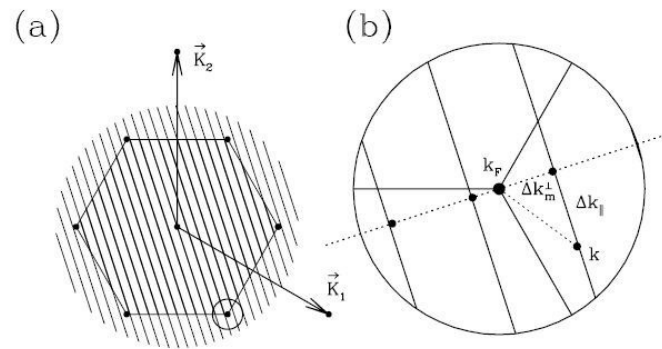
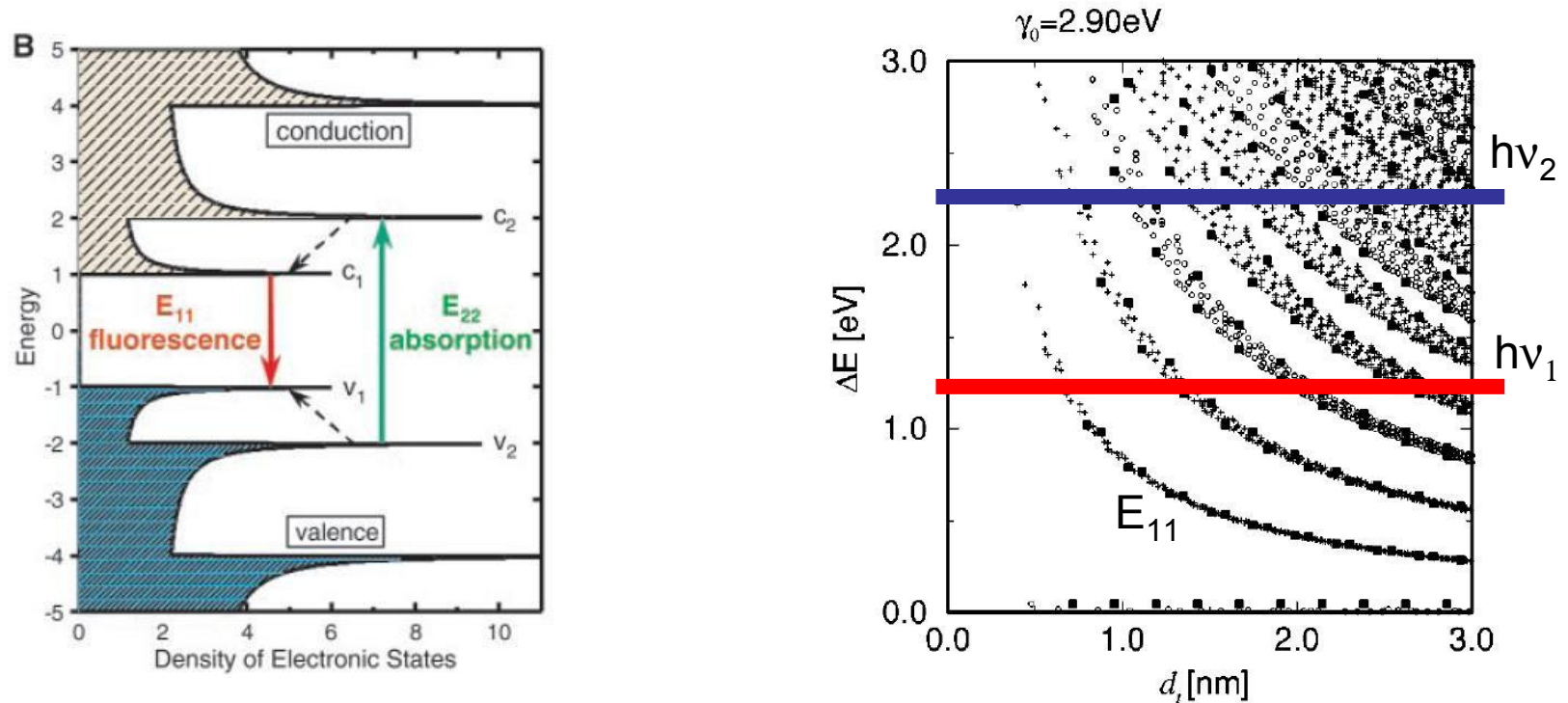


(Fig: Bachilo et al., Science **268** (2002))



Optical properties, van Hove singularities (vHs) and Kataura's plot (see Lecture by T. Hertel)

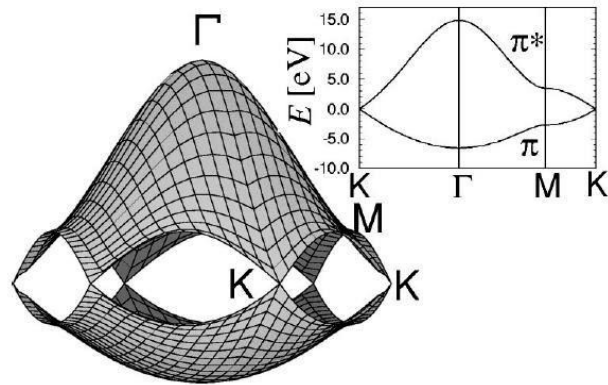
Early interpretation of optical data identified the absorption peaks with the energy difference E_{ij} between vHs in the unoccupied and occupied bands.



For high energy transitions, broadening of the $1/d_t$ lines: the linear approximation not so exact and the transition energies depend also on the (n,m) indices.

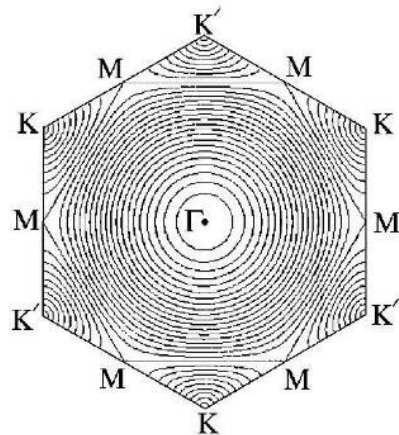
Kataura et al., Synthetic Metal **103**, 2555 (1999); Saito et al., PRB **61**, 2981 (2000); Popov+Henrard, PRB **70**, 115407 (2004); etc.

Trigonal warping and broadening of E_{ii} lines in Kataura's plot

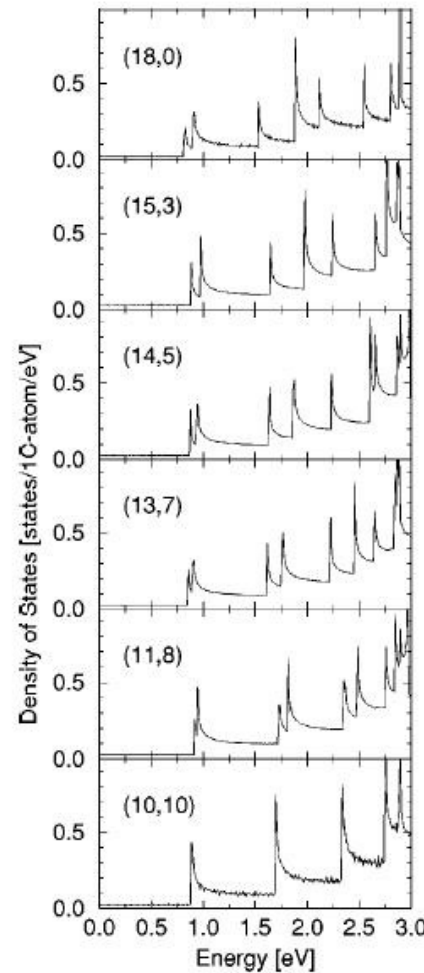


Energy bands are not linear away from E_F

$$E(k) \neq \pm v_F |k - k_F| \quad \text{if} \quad E(k) - E_F > \varepsilon$$



Iso-energy levels around K become trigonal when crossing MM lines.



Observe splitting of vHs peaks (maximum for metallic zigzag tubes).

(nanotubes of similar diameter 1.3-1.4 nms)

**As a result, E_{ii} do not depend only on tube diameter for high-energy transitions !
Complicate the reading of the Raman, optical, etc. data.**

Deviations from band folding: curvature effects

The \mathbf{k} -point at which valence and conduction bands do overlap in graphene is conditioned by the annulation of:

$$H_{AB}(\mathbf{k}) \sim \gamma_1 + e^{-ik \cdot \mathbf{a}_1} \gamma_2 + e^{-ik \cdot \mathbf{a}_2} \gamma_3$$

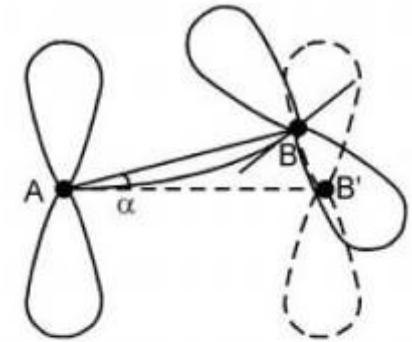
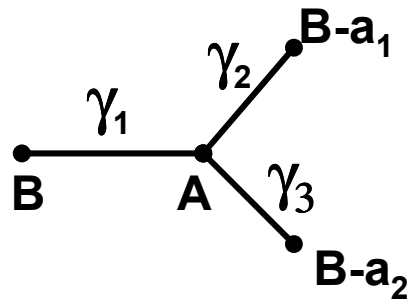
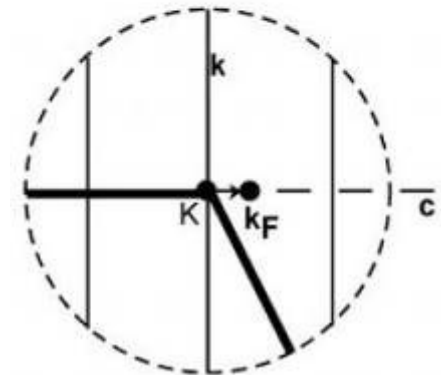


(Fig: Ouyang et al., Science 2001)



In planar graphene, $\gamma_1 = \gamma_2 = \gamma_3 = \gamma_0 \Rightarrow$ bands cross at K

In nanotube, bonds parallel and perpendicular (or with an angle)

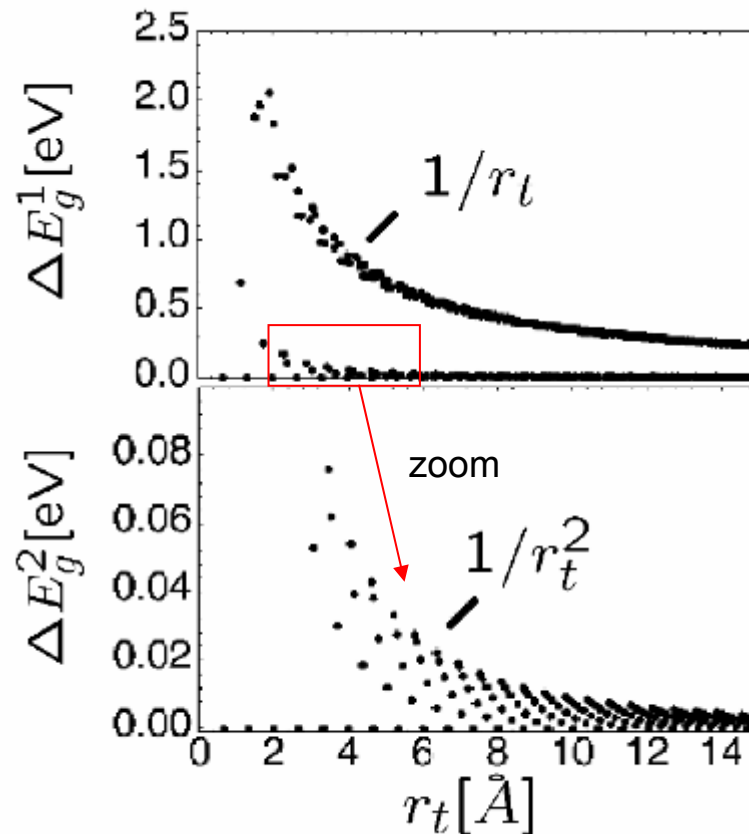
with the tube axis are non-equivalent $\Rightarrow \gamma_1 \neq \gamma_2 \neq \gamma_3$

➔ The \mathbf{k} -point which cancels $H_{AB}(\mathbf{k})$ is shifted away from the zone-corners \mathbf{K} .

Armchair tube : this point is shifted along an allowed line \Rightarrow remains metallic
Metallic non-armchair: shifted off the allowed lines \Rightarrow opens a small band gap

Curvature effects and secondary gaps in « metallic » non-armchair tubes

Theory



$$\Delta E_g^2 = \frac{3\gamma_0 a_{cc}^2}{4d_t^2} \times \cos(3\theta)$$

(chiral angle; $\theta=0$ for zigzag)

Experiment

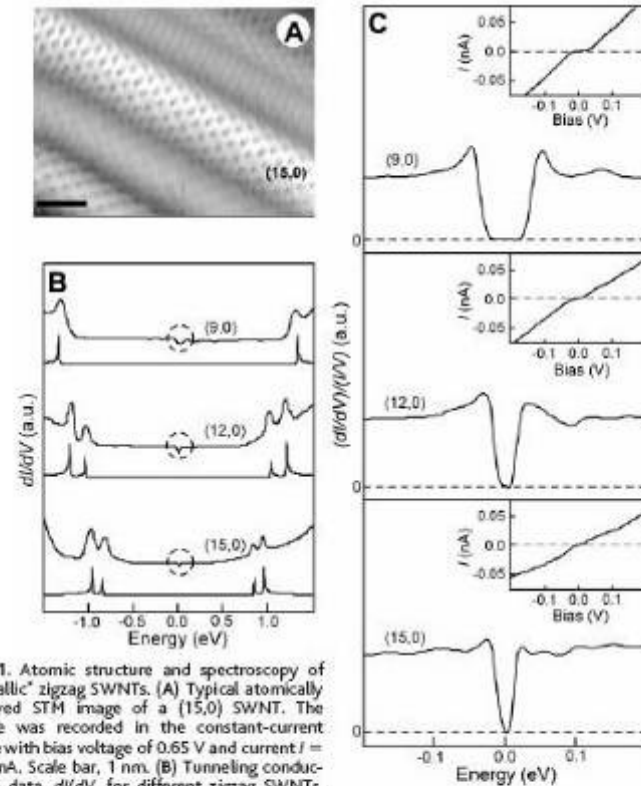
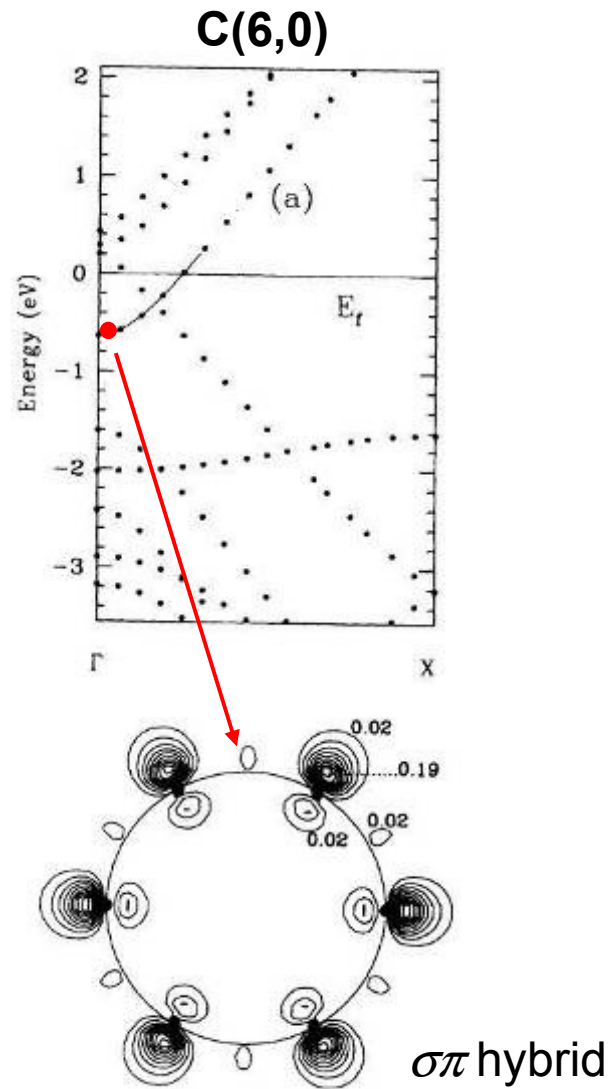


Fig. 1. Atomic structure and spectroscopy of 'metallic' zigzag SWNTs. (A) Typical atomically resolved STM image of a (15,0) SWNT. The image was recorded in the constant-current mode with bias voltage of 0.65 V and current $I = 0.15$ nA. Scale bar, 1 nm. (B) Tunneling conductance data, dI/dV , for different zigzag SWNTs, with corresponding calculated DOS shown below each experimental curve (a.u., arbitrary units). The data were recorded as the in-phase component of I directly by a lock-in amplifier with a 7.37-kHz modulation signal of 2 mV peak-to-peak amplitude to the bias voltage. The new features in the low-energy region of the (9,0), (12,0), and (15,0) tubes are highlighted by dashed circles. (C) Typical high-resolution normalized conductance $(dI/dV)/(I/V)$ curves and measured $I-V$ curves (insets) for (9,0), (12,0), and (15,0) tubes, respectively. The $(dI/dV)/(I/V)$ curves were calculated from dI/dV and $I-V$ data.

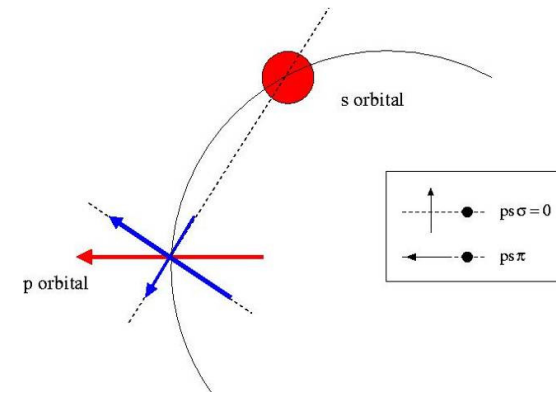
Kane and Mele, PRL **78**, 1932 (1997)
Kleiner and Eggert, PRB **64**, 113402 (2001)

Ouyang *et al.*, Science **27**, 292 (2001)

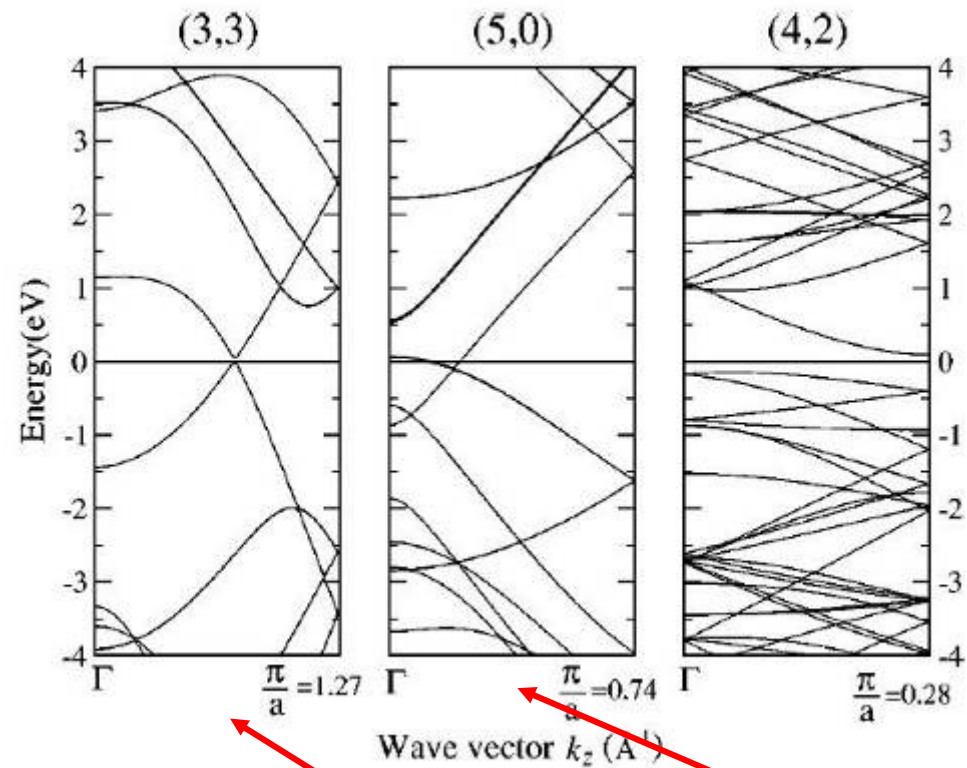
σ – π hybridization in small diameter tubes



Blase et al., PRL **72**, 1878 (1994)



Ordejón et al. PRB **66**, 155410 (2002)



The effect is small for armchair, important for zigzag

A (ridiculously) tiny note on symmetries in nanotubes

T. Vukovic *et al.*, Phys. Rev. B **65**, 045418 (2002)

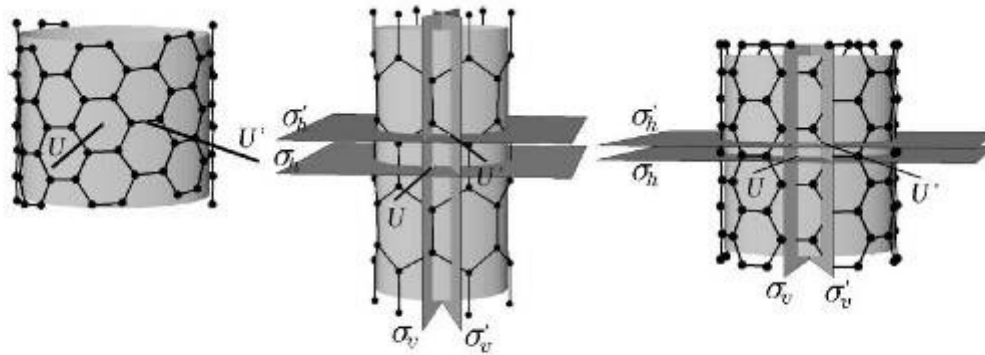
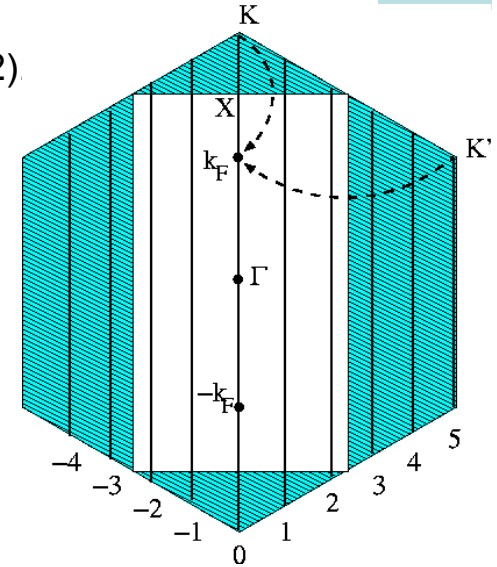


FIG. 2. Symmetries of the single-wall nanotubes: (8,6), (6,0), and (6,6). The horizontal rotational axes U and U' are symmetries of all the tubes, while the mirror planes (σ_v and σ_v'), the glide plane σ_h' , and the roto-reflectional plane σ_h are symmetries of the zigzag and armchair tubes only. The line groups are $T_{148}^{31}D_2$ for (8,6), and $T_{12}^1D_{6h}$ for the other two tubes.



Translation group => « $k_{||}$ Bloch vector » are quantum numbers

The allowed line « q »-index is also the azimuthal quantum number
($\exp(iq\theta)$ phase factor « around » the tube).

In achiral tubes (zigzag, armchair) reflexion and glide planes => parity number

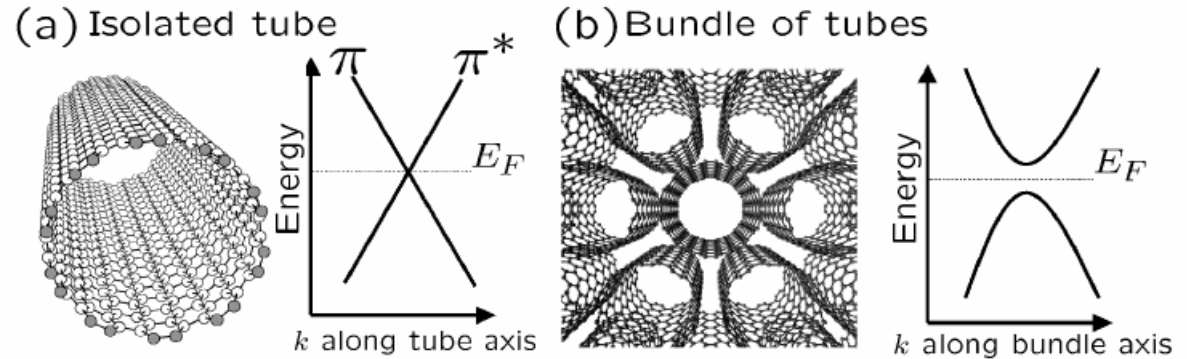
A perturbation mixes two subbands with (α, β) quantum number if it has an γ -component such that $\alpha - \beta \pm \gamma = 0$

The effect of a perturbation (squashing, tube-tube interaction, substrate-tube Interaction, σ - π hybridization, electric field (gate voltage), optical perturbation, etc. can be analyzed with group theory to know which bands will be affected.

Tube-tube interactions in a SWNTs bundle

Tube-tube interactions break the tube symmetries $\Rightarrow \pi-\pi^*$ repulsion and opening of a gap (~ 0.1 eV) in metallic (10,10)

Bundling can also reduce gap of semiconducting tubes through « lateral » dispersion.

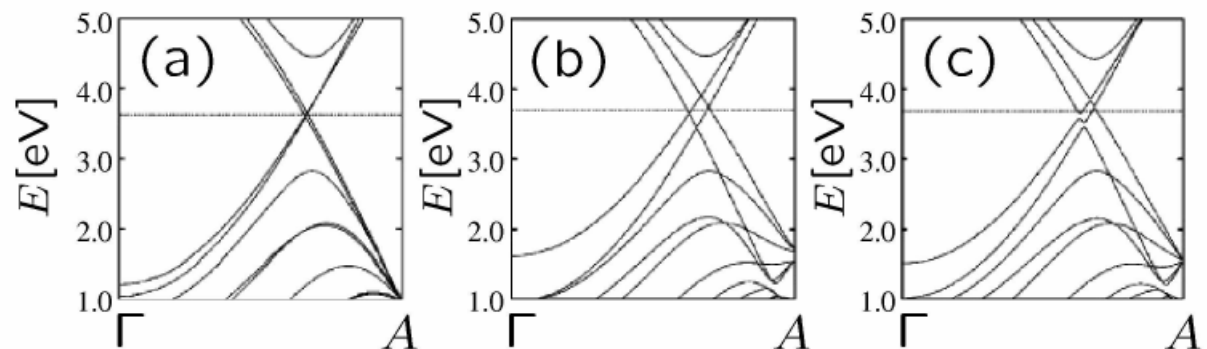


Delaney *et al.*, *Nature* **391**, 466 (1998)
 Charlier *et al.*, *Europhys. Lett.* **29**, 43(1995)
 Reich *et al.*, *PRB* **65**, 155411 (2002)

(Exp: Ouyang *et al.*, *Science* **292**, 702 (2001))

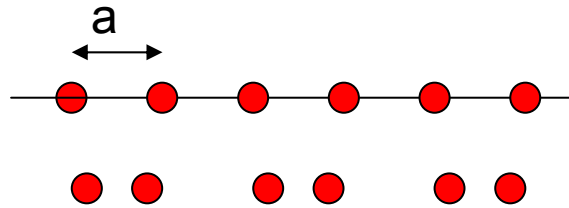
Tube-tube interaction in a MWNTs

Bilayer tube: rotating the inner tube (5,5)@(10,10)



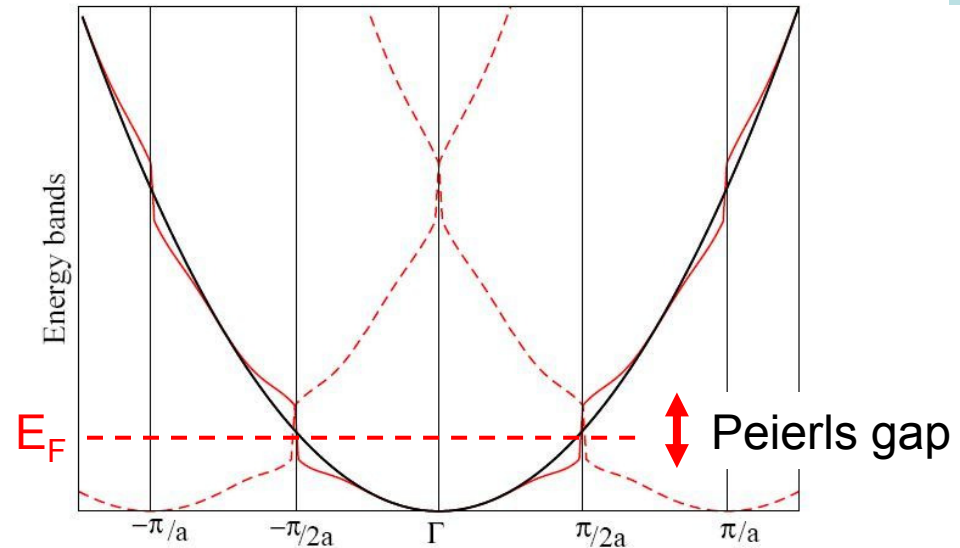
Kwon and Tománek, *PRB* **58**, 16001 (1998)
 Lambin *et al.*, *Comput. Matter Sci.* **2**, 350 (1994)

Peierls distortion in CNTs



**Dimerization of an atomic chain
with one electron per site.**

(Kittel, Intro to Solid State Physics)



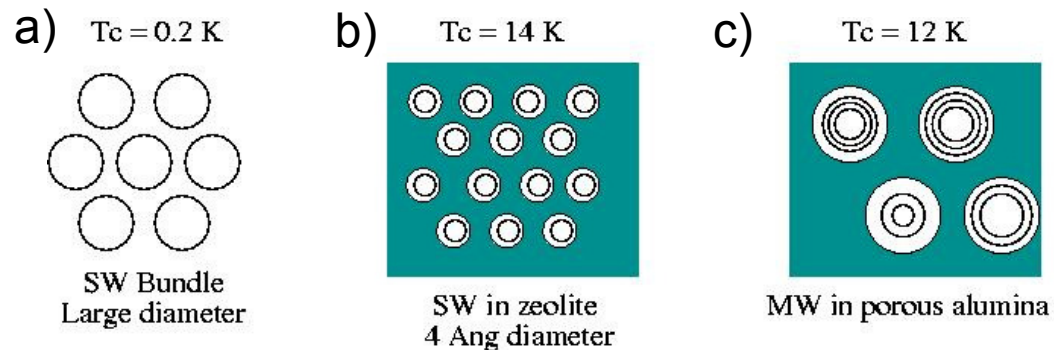
General theorem : metallic 1D systems are unstable at low temperature with respect to $2k_F$ momentum lattice perturbation. It always happens : the real question is « what is the transition temperature T_{CDW} ?? » (CDW=charge density wave)

The transition temperature depends exponentially on the strength of the electron-phonon deformation potentiel associated with the lattice deformation
=> difficult to calculate it with accuracy and large dispersion in theoretical values.

(Mintmire *et al.*, PRL 1992; Saito *et al.*, APL 1992; Figge *et al.*, PRL 2001; De Martino and Egger, PRB 2003; Sédéki *et al.*, PRL 2002)

T_{CDW} much smaller than room temperature except for small diameter nanotubes ($D = 4 \text{ \AA}$) with room temperature transition predicted by ab initio calculations.

(Bohnen *et al.*, PRL 2004; Connétable *et al.*, PRL 2005.



Experiments:

- a) Kociak *et al.*, PRL 2001
- b) Tang *et al.*, Nature 2001
- c) Haruyama *et al.*, PRL 2006

Theory:

Sédéki *et al.*, PRB 2002;
 Kamide *et al.* PRB 2003;
 González 2002; Alvarez+González, 2003;
 González+Perfetto, 2005.

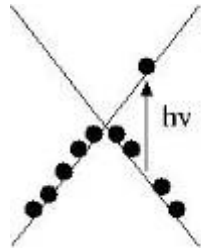
The superconducting order is difficult to observe in 1D systems for several reasons:

- Competition with the CDW instability : the electron-phonon coupling channels can either induce CDW order or SC order (cf. BCS approach). Both instabilities are not compatible. (T.Giamarchi, Quantum physics in One Dimension, Oxford Science Pubs., 2004)
- Long-range order at finite T is impossible in 1D systems due to thermal fluctuations (see: Mermin and Wigner, PRL 17, 1133 (1966))
- Even at $T=0 \text{ K}$, quantum fluctuations due to quantum phase slip induce a non-zero resistivity unless $T=0 \Rightarrow$ smooth decay of resistivity below T_c (Langer+Ambegaokar, PR **164**, 498 (1967))

T_c increases with decreasing diameter: strength of the e-ph coupling increases due to curvature effects ($pp\pi \Rightarrow pp\sigma$ coupling) and normalisation ($1/D$ and $1/D^2$ dependence) (Benedict *et al.*, PRB **52**, 14935 (1995))

Bundling favors superconductivity as it reduces the 1D character (better screening of the electron-electron repulsion, Josephson coupling between tubes, etc.)

Luttinger liquid transition in CNTs (effect of electron-electron interactions)



Standard picture of an electronic excitation: one electron is excited, the others do not move.



Can you really pull on a mass without moving the other ones ?

Coulomb interaction is strong in electron gaz: scattering of one electron should affect collectively all the others

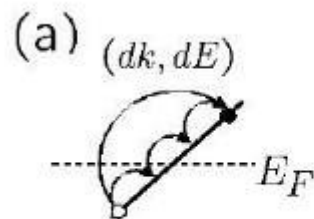
Collective excitations: plasmons, spinons

In 3D systems, Pauli principle says that close to E_F , single-particle excitations are possible:

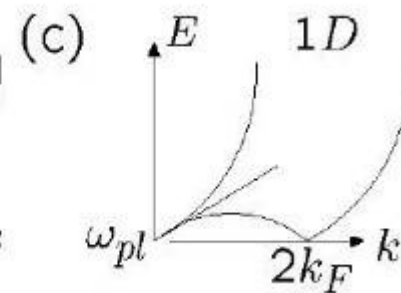
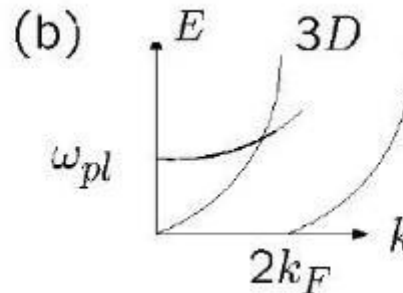
$$\Rightarrow 1/\tau^{ee} \approx (E - E_F)^2 \text{ (Fermi liquid theory, Nozières-Pines, 1964).}$$

This is no longer true in 1D: low energy excitations are collective excitations (plasmons, spinons)

\Rightarrow Luttinger liquid behavior (Tomonaga (Nobel prize 19xx), Luttinger)



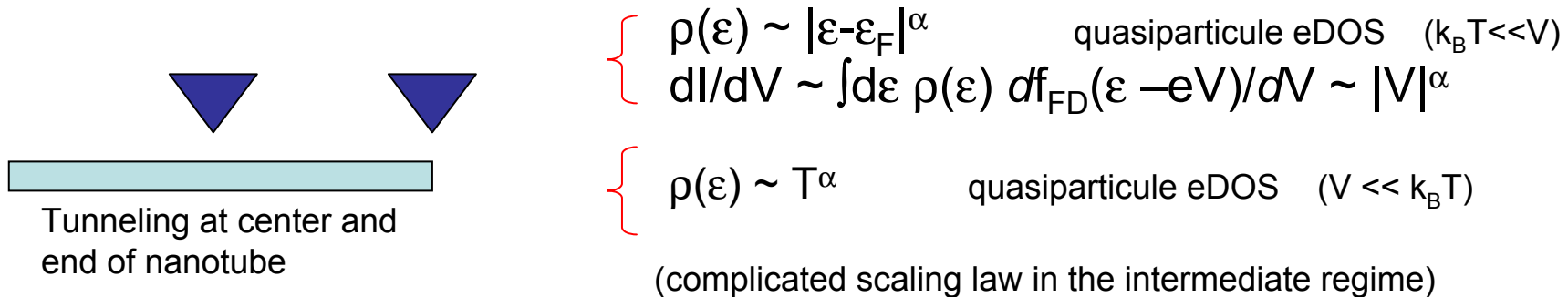
Single excitation decay in n-excitations
(linearity of bands makes conservation of energy and momentum preserved)



In 3D, single particle and plasmons are decoupled.
In 1D, they are resonant.

Signature of the Luttinger liquid behavior: transport properties

Tunneling rate into LL is suppressed at low voltage and temperature as a power law.



$$\alpha_{\text{end}} = (1/g - 1)/4$$

$$\alpha_{\text{bulk}} = (1/g + g - 2)/8$$

The exponent α depends on the electron-electron interaction parameter g ($0 < g < 1$ repulsive interactions; $g = 1$ Fermi liquid)

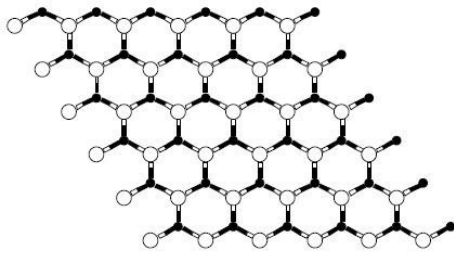
However, difficult to distinguish at low T the LL behavior with Coulomb blockade effects (Egger+Gogolin, PRL **87**, 066401 (2001))

Egger and Gogolin, PRL **79**, 5082 (1997); Kane *et al* PRL **79**, 5086 (1997); Egger, PRL **83**, 5547 (1999); Eggert PRL **84**, 4413 (2000); Lopez-Sancho *et al.* PRB **63**, 165419 (2001); Mora *et al.* PRB, submitted (2006) M. Bockrath *et al.*, *Nature* **397**, 598 (1999); O. M. Auslaender *et al.*, *Phys. Rev. Lett.* **84**, 1764 (2000); Z. Yao, *et al.*, *Nature* **402**, 273 (1999); Gao *et al* PRL **92**, 216804 (2004); Lee *et al.* PRL **93**, 166403 (2004)

Note: A spin/charge density waves separation has been evidenced as well (Lee *et al.* PRL **93**, 166403 (2004)), providing a strong proof for a possible LL behavior.

Planar and nanotubes *h*-BN structures

BN planar sheet



BN zigzag tube



$$\det \begin{pmatrix} \mathcal{H}_{AA} - E & \mathcal{H}_{AB} \\ \mathcal{H}_{BA} & \mathcal{H}_{BB} - E \end{pmatrix} = 0$$

$$\mathbf{H}_{AA} \neq \mathbf{H}_{BB}$$

At **K**, where $\mathbf{H}_{AB}=0$, opening of an ionicity gap: $E_{\text{gap}} = |\mathbf{H}_{AA} - \mathbf{H}_{BB}|$

BN tubes synthesis: Loiseau et al. PRL **76**, 4737 (1996); Chopra et al., Science **269**, 966 (1995); etc.

BN tubes theory: Rubio et al., PRB **49**, 5081 (1994) ; Blase *et al.*, Europhys.Lett. **28**, 335 (1994);
ibid. PRB **51**, 6868 (1995).

Arnaud et al., PRL **96**, 026402 (2006)

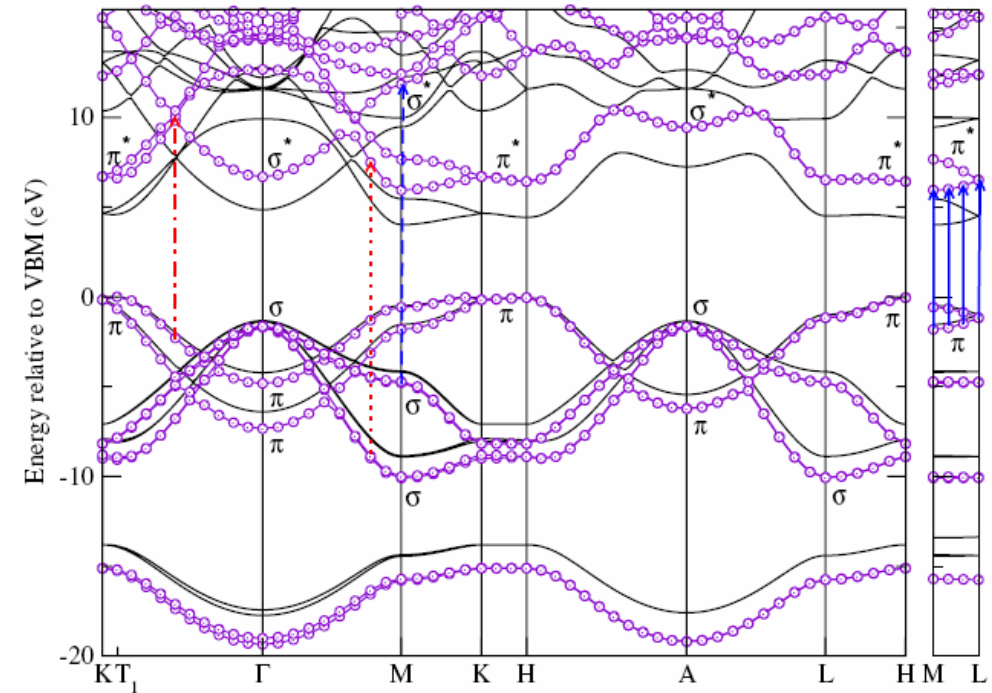


FIG. 1 (color online). Calculated electronic band structure along high-symmetry lines for bulk hexagonal boron nitride. The thin solid lines display the LDA results while the solid lines with open circles show the *GW* approximation results. The energy scale is relative to the top of the valence band maximum (VBM) located at the T_1 point near *K* along the Γ -*K* high-symmetry direction.

Photoluminescent h -BC₂N systems

Experimental evidence of visible range photoluminescent character.

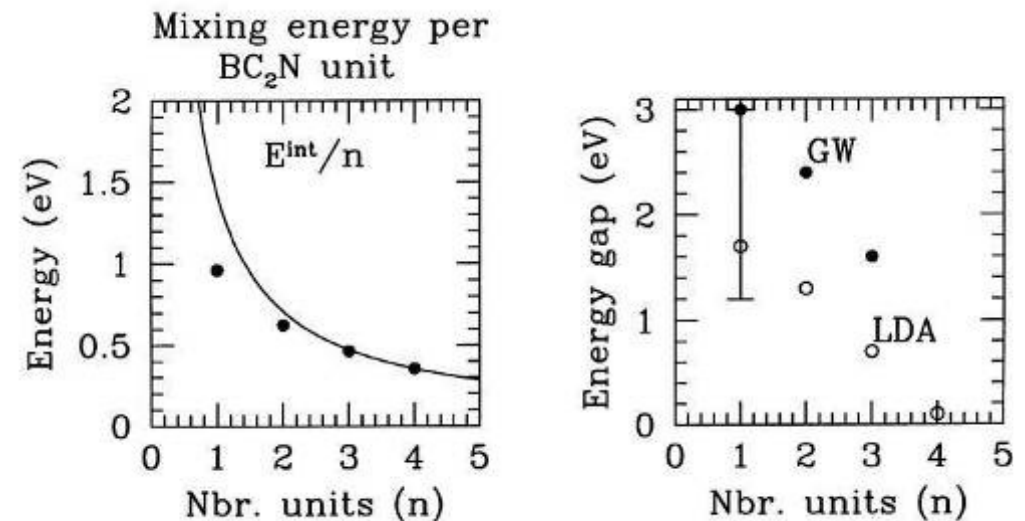
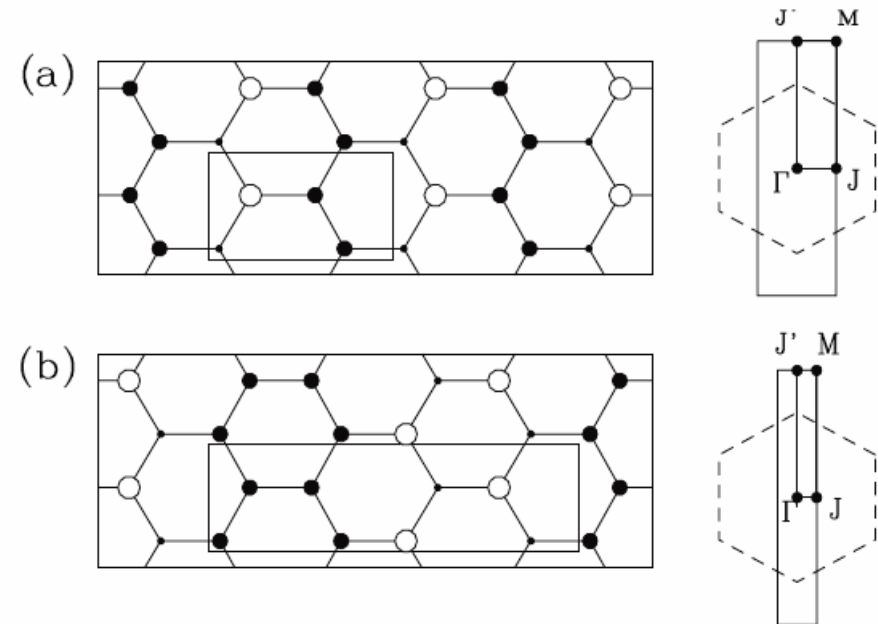
Watanabe et al., PRL **77**, 187 (1996)
Chen et al., PRL **83**, 2406 (1999)

Theory: tendency towards segregation in large pure C or BN domains.

Liu, *et al.*, PRB **39**, 1760 (1988).
Blase et al., APL **70**, 197 (1997)
Blase et al., Appl. Phys. A **68**, 293 (1999)
Mazzoni et al., PRB **73**, 073108 (2006)

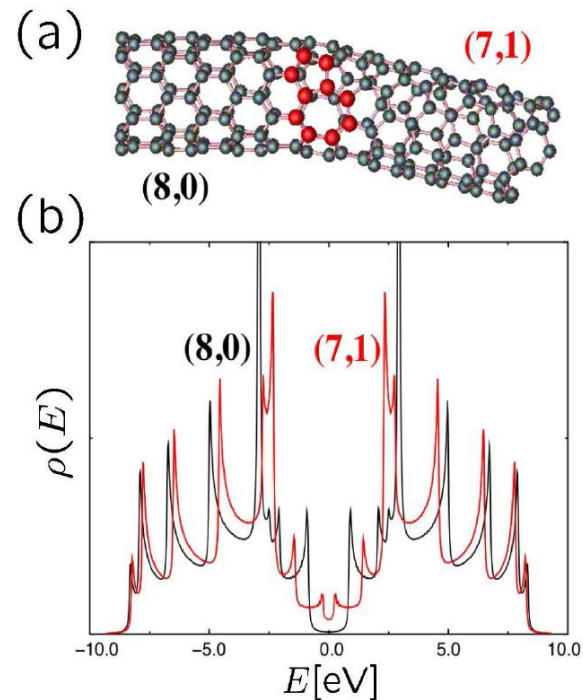
Upon segregation, band gap goes from zero to 3 eV (visible range 1.8-3 eV)

Blase et al., Appl. Phys. A **68**, 293 (1999)
Mazzoni et al., PRB **73**, 073108 (2006)



Addenda 1: tube-tube junctions

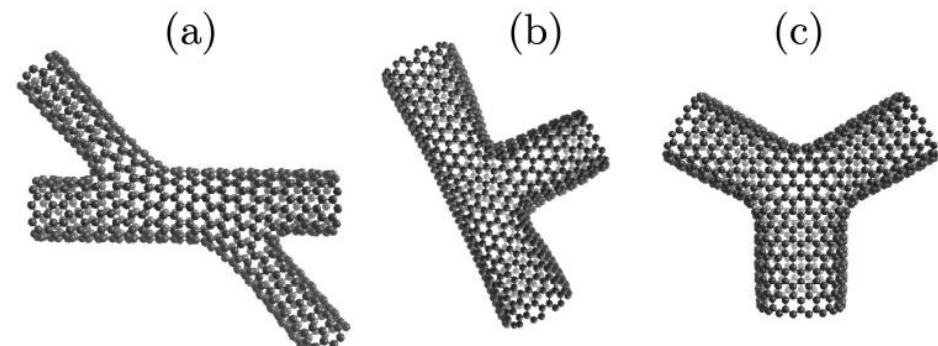
(5,7) defects can “branch” two tubes with different chiralities, that is different band gaps => rectifying junctions



Dunlap, PRB 1994; Lambin et al., CPL 1995;
Saito et al., PRB 1996; Chico et al., PRL 1996.

Exp: Yao *et al.*, *Nature* **402**, 273 (1999);
Ouyang *et al.*, *Science* 291, 97 (2001).

Electron beam irradiation can weld tubes to form X,Y or T junctions.



Terrones *et al.*, *Science* 2000; PRL 2002;
Meunier *et al.*, *APL* 2002.